Reversible catalysis

Vincent Fourmond, Nicolas Plumeré, Christophe Léger

This is a post-peer-review, pre-copyedit version of an article in press. Please cite: Fourmond, V., Plumeré, N & Léger, C. Reversible catalysis. Nat. Rev. Chem. doi: 10.1038/s41570-021-00268-3 (2021)

Reversible catalysis

Vincent Fourmond [1], Nicolas Plumeré [2], and Christophe Léger [1*]

[1.] Laboratoire de Bioénergétique et Ingénierie des Protéines. CNRS, Aix Marseille Université, Marseille, France

[2.] Campus Straubing for Biotechnology and Sustainability, Technical University Munich, Schulgasse 22, 94315, Germany.

* Email: leger@imm.cnrs.fr

Abstract | We describe as "reversible" a catalyst that allows a reaction to proceed at a significant rate in response to even a small departure from equilibrium, resulting in fast *and* energy efficient chemical transformation. Examining the relation between rate and thermodynamic driving force is the basis of electrochemical investigations of redox reactions, which can be catalysed by metallic surfaces and synthetic or biological molecular catalysts. How rate depends on driving force has also been discussed in the context of biological energy transduction, regarding the function of biological molecular machines in which chemical reactions are used to produce mechanical work. We discuss the mean-field kinetic modeling of these three types of systems (surface catalysts, molecular catalysts of redox reactions, and molecular machines), in a step towards the integration of the concepts in these different fields. We emphasize that reversibility should be distinguished from other figures of merit, such as rate or directionality, before its design principles can be identified and used in the engineering of synthetic catalysts.

Introduction

Both life[1] and industry[2] rely on energy conversion, which remains a challenge today. This is particularly true in the solar fuels field, where catalysts are needed to efficiently store in the form of chemicals (such as dihydrogen) the energy collected from intermittent sources.

Optimal energy conversion is reached when the system functions near equilibrium, under conditions of thermodynamic reversibility, but real, non-ideal systems function under non-equilibrium conditions and dissipate as heat a fraction of the input energy.

The molecular catalysts of redox reactions that are very active in response to even a small departure from equilibrium have been called "reversible"[3–5] (although this term is used with various other meanings, which may lead to confusion, see Box 1). The same definition could also be used for non-redox catalysts. Catalytic reversibility provides an advantage when the energy that is input in the system must not be wasted, and understanding why some catalysts perform reversibly is required to improve the design of those that do not.

Here we mostly focus on the catalytic activation of small molecules and on biological energy transduction, and we discuss the literature on the kinetic modeling of various types of catalysts: redox enzymes, synthetic molecular catalysts and surface catalysts of redox reactions, and biological machines. We observe that the question of the relation between rate and driving force is not asked in the enzymology and homogeneous catalysis literature ; in contrast, it recently became central in the context of molecular catalysis of redox reactions, but it is answered in a manner which we think should be revisited. Central to the discussion in this paper is the distinction between the various figures of merit of a catalyst and the existence of tradeoffs between them: we begin by discussing

rate and directionality (or "catalytic bias"), before examining reversibility. Each of these properties has been discussed with respect to the function of surface catalysts, molecular redox catalysts and biological motors, but differences in vocabulary have blurred useful connections between these research fields.

Rate

The most obvious measurement of the performance of a catalyst is its specific activity: the rate of the chemical transformation per catalyst mass, or per molecule (the turnover frequency for molecular catalysts or the "flux" in molecular motors), or the rate per geometric surface, or site on a surface. Catalysts increase the rate of a reaction by changing the reaction mechanism, and breaking it up into a series of steps that have low activation energies. This is commonly summarized by the idea that catalysts flatten the "energy landscape" of the reaction, although when this familiar expression is used, whether flatness relates to the energies of the catalytic intermediates or also considers the barriers between them is not always explicit.

Some enzymes are extremely active[6], with specificity constants (the effective bimolecular rate constant k_{cat}/K_M) approaching the upper limit of 10^9 $s^{-1}M^{-1}$ (ref [7]), but the specificity constant of an enzyme is usually much smaller, around 10^5 $s^{-1}M^{-1}$, and a maximal turnover frequency k_{cat} of 10 s^{-1} is very common[8]. Biological motors can also function at high speed, typically several hundreds of complete cycles per s; for example, the kinesin molecule (figs 3a and 1f) uses the free energy of ATP hydrolysis to run along microtubules in a specific direction at up to 2 µm/s (ref [9]).

Directionality

Another property of catalysts is their "directionality", which measures whether the catalyst allows faster reaction in one direction of the reaction than in the other. Of course the *direction* of a chemical reaction only depends on thermodynamics (figure 2a), but an *intrinsic* directionality of the catalyst can be defined by calculating the ratio of two rates measured under conditions chosen to make the reaction progress forward or backward (large and either positive or negative $\Delta_r G$). The ratio of these rates, measured under distinct conditions, is not an equilibrium constant[10].

The terms "(uni/bi)directional"[4,11,12], "catalytic bias"[13–22] or "catalytic preference"[3] have been used to describe this catalytic property by the community working on hydrogenases (the enzymes that oxidize and evolve H_2). Enzymologists describe as "one-way" the enzymes that effectively catalyse the reaction in only one direction of the reaction[23,24].

It seems that the vast majority of *synthetic* molecular catalysts only work in one direction of the reaction; two examples of synthetic *bidirectional* molecular catalysts are shown in figure 1c-e. Some surface catalysts and biological motors also "prefer'' one direction. For example platinum is the best pure metal oxygen reduction reaction (ORR) electrocatalyst but does not perform well for the oxygen evolution reaction (OER)[25] and MoS_2 catalysts are much better for the hydrogen oxidation reaction (HOR) than the hydrogen evolution reaction (HER)[26]. Biological motors are also characterized by a catalytic bias (although not with this terminology): for example, kinesin (fig 3a) backtracks only at a very reduced speed in response to a large backward mechanical load (fig 2c)[27–29].

One explanation of the bias of redox catalysts in one direction is based on the idea that their structure is not the same under oxidative and reductive directions. In the case of non precious metals and metal alloys, surface oxidation occurs under OER conditions, with the formation of surface oxides and hydroxides that are not present under the reductive conditions required for the ORR[30,31]. Regarding metalloenzymes, a slow redox-driven structural modification of the active site can also result in a loss of activity under very oxidizing or reducing conditions[32]. This is common for

hydrogenases: the active site of NiFe hydrogenases can be over-oxidized into various dead-end species[33] and certain FeFe hydrogenases[34–36] also inactivate under moderately oxidizing conditions, which prevents H_2 oxidation and effectively biases the enzyme in the reductive direction.

A distinct explanation of the origin of the catalytic bias is related to kinetics[3]. It may happen that a bidirectional step that controls the maximal rate in both directions of the catalytic cycle has an equilibrium constant different from one, therefore making maximal turnover faster in one particular direction. Or two distinct steps may independently control the rates in the two directions of the reaction. These two situations have been observed for HER and HOR in two different hydrogenases[14,15].

For enzymes whose mechanism is ordered (figure 1a), the kinetic parameters in the two directions of the reaction and the equilibrium constant are linked by a Haldane equation[23]. For example, in the case of an enzyme that transforms a single substrate S into a single product P, the forward and backward maximal rates (v_{max}^{f} and v_{max}^{b} respectively, whose ratio measures the catalytic bias), the substrate and product Michaelis constants (K_M^S and K_M^P) and the equilibrium constant obey the relation:

$$K_{\mathrm{eq}} = \frac{[\mathrm{P}]_{\mathrm{eq}}}{[\mathrm{S}]_{\mathrm{eq}}} = \frac{v^f_{\mathrm{max}} K^{\mathrm{P}}_M}{v^b_{\mathrm{max}} K^S_M} \quad (1)$$

More complex kinetic schemes (each scheme considering the binding and release of more than one substrate and product, and a specific order of the events in the catalytic cycle) give more complex Haldane equations[37,38]. An "electrochemical Haldane equation" for the molecular catalysts of two-electron reactions is discussed below (eq 7).

In the inorganic chemistry field, there are very few examples of catalysts that work both ways. The so-called Ni "DuBois catalysts", initially from the Pacific Northwest National Laboratory, oxidize and/or produce H_2 at significant rates[4,39–42]. These catalysts are mononuclear nickel complexes, with bioinspired proton-transferring ternary amines which have been modified with various substituents (R and R' in figure 1d). Their intrinsic directionality has been related to the free energy of reaction with hydrogen[43], negative $\Delta_r G$ favoring the activity in the direction of H_2 oxidation[44], and thermoneutrality allowing catalysis to proceed both ways[39]. The relation between this free energy of reaction and the catalytic bias has not yet been given justification by a kinetic model.

A complication in the comparison of the rates of the reaction in the two directions is that the forward and backward series of steps may be distinct. Indeed, the principle of microscopic reversibility does not impose that the reaction pathways that are taken under distinct conditions should be the same (however, it does impose relations between the rate constants around a cycle, even in a productive cycle[45,46]). We therefore distinguish ordered mechanisms, in which the forward and backward reactions follow the same catalytic pathway either clockwise or counter-clockwise (figure 1a), and "branched mechanisms"[3] (called "random mechanisms" in enzymology[47]), which occur if there are branch points along the catalytic reaction pathways, where alternative steps (such as electron and proton transfers) compete (figure 1b). A branched mechanism can switch between paths as the experimental conditions change: distinct pathways may dominate under distinct experimental conditions, although any change must happen continuously as the experimental conditions are varied, going through conditions where the two pathways coexist[3]. Regarding the transfers of electrons and protons, concerted steps may also occur[48,49].

That the DuBois complexes exist in many different states allows for a variety of pathways (figure 1e), each being defined by a particular sequence of redox steps ("E") and chemical steps ("C"). Regarding the R=cyclohexyl, R'=phenyl complex, which under certain conditions shows about equal catalytic currents for H_2 oxidation and evolution[42], it is proposed that the two reactions occur near the

equilibrium potential along an ECECCCC pathway (a↔b↔c↔e in figure 1e). Under more reducing conditions, H_2 production occurs by an EECCCC pathway (b→d→e) because the reduction step b→d becomes fast and outcompetes the protonation step b→c. H_2 oxidation at high potential may occur along a distinct pathway in which intramolecular isomerization of the H_2 addition product (g→h) allows the catalyst to be oxidized (h→i) prior to removal of the first proton (i→c→b→a)[3].

Uncoupling occurs when a branched mechanism includes futile cycles. In that case the function of the system cannot be defined by a unique balanced equation. Uncoupling between chemistry and mechanical work occurs e.g. when kinesin stops in response to a stall force but keeps hydrolysing ATP (instead of synthesizing it, which would be the reverse of the forward walk)[28,50–52]. In contrast, F_0F_1-ATP synthase is an example of a biological motor that, independently of any consideration on rate, fully uses the free energy of a proton gradient to synthesize ATP[53]. The same distinction is relevant in the case of chemical catalysts. For example artificial CO_2 reduction catalysts produce a mixture of products (including H_2)[54,55], whereas the enzymes that reduce CO_2 produce pyruvate, CO, or formate in a very specific manner. But not all enzymes are perfect in this respect. For example, the enzyme nitrogenase, which performs the very difficult reduction of N_2 into NH_3 under mild conditions, wastes some reducing equivalents in futile cycles, by evolving more than one H_2 molecule per N_2 being reduced [56].

Reversibility

Whereas directionality is concerned with the rates measured under conditions of extreme driving force, catalytic reversibility is a figure of merit that reflects the dependence of the turnover frequency on the thermodynamic driving force under near equilibrium conditions, as illustrated in figure 2a.

This dependence of rate on thermodynamics may sound like an abstract concept because the driving force is in many experimental situations a parameter that cannot be readily varied. A rare example in the enzymology literature is Cees Veeger's measurement of the rate of the HER by the enzyme hydrogenase, with reduced methyl viologen (MV) as electron donor, as a function of the ratio of oxidized over reduced viologen (figure 2b)[57]. The latter defines the Nernst potential of the $MV_{ox/red}$ couple and thus the free energy of the overall reaction between H^+ and MV_{red} (assuming constant H_2 pressure and pH).

In the case of chemical transformations, the driving force is simply the free energy of the reaction; for molecular machines the driving force is the difference between the "input" energy (e.g. the free energy of ATP hydrolysis) and the fraction of that energy that is transduced (e.g. in the form of mechanical work)[9]. Figure 2c shows the velocity of kinesin as a function of the backward force that is applied. At equilibrium the stall force compensates for the input free energy of ATP hydrolysis and the motor stops[28]. There have been many measurements of how the velocity of various motors depends on force and/or on the input free energy (set by the ATP concentration)[58]; see e.g. ref [59] for the effect of torque on the rate of ATP synthesis by the F_1 ATP-synthase subcomplex.

In only one type of experiment is it easy to measure the rate of a chemical reaction as a function of driving force: the electrochemical investigation of redox reactions, including the characterization of the catalysts of these reactions. If the redox reaction that is considered takes or gives electrons to an electrode (figure 2d-h), the sign of the current that flows through the electrode indicates the direction of the reaction (oxidation versus reduction) and its magnitude is proportional to the rate of the reaction. The overpotential η that is applied, defined here by $\eta = E - E_{eq}$, can be positive or negative, and it is proportional to minus the free energy $\Delta_r G$ of the redox reaction. A negative overpotential, or positive free energy, drives the reaction in the backward (i.e. reductive) direction. Equilibrium is reached when the electrode potential equates the Nernst potential of the

corresponding redox couple (E_{eq}), as e.g. observed in electrochemical studies of redox enzymes that reversibly convert H^+ and H_2,[60–62] succinate/fumarate,[63,64] CO_2/CO,[65] CO_2/formate,[66] NADH/NAD^+,[67] or tetrathionate/thiosulfate[68]. In a typical voltammetric experiment, the electrode potential is swept up and down and the current response is monitored; the results are usually displayed in a plot of current against potential called voltammogram. If one ignores a number of complications resulting from the possible effects of mass transport towards the electrode,slow (in)activation of the catalyst etc.[69], experimental voltammograms such as those in figures 2i-n can be seen as plots of rate against thermodynamic driving force. Voltammograms, whose shape and magnitude depend on experimental parameters, can be examined in the framework of kinetic models to benchmark the catalysts (e.g. determine their turnover frequencies) and to study their mechanisms[70–72].

We and others have described as "reversible" a bidirectional catalyst that allows a reaction to proceed at a significant rate in response to even a small departure from equilibrium (see Box 1). In the particular case of a redox catalyst: one that gives a significant current even at a small overpotential[3–5] (figure 2m-n). Only bidirectional catalysts can function reversibly. Indeed, a reaction rate can only change smoothly as a function of $\Delta_r G$, and therefore it cannot happen that e.g. the rate is small and negative when $\Delta_r G$ is small and negative, and abruptly large and positive when $-\Delta_r G$ is small and positive. But a bidirectional catalyst may also function irreversibly, if a significant positive or negative $-\Delta_r G$ is needed to drive the reaction in one direction or the other, as illustrated by the voltammogram in figure 2i, or fig 2l for the R=cyclohexyl, R'=pyridizine DuBois catalyst, or fig 8 in ref [73] for a peculiar example of FeFe hydrogenase performing bidirectionally and irreversibly.

The benchmarking of catalytic reversibility

The measurement of catalytic reversibility is very different for electrocatalysts (i.e. *surface* catalysts) and molecular catalysts, because the typical shapes of the current/potential responses are different. This is one of the reasons why the conclusions from one field cannot be simply used in the other.

The electrochemical response of electrocatalysts is essentially an exponential increase in current as the overpotential increases; in the simplest cases, and counting the oxidation current as positive:

$$i = i_0 \left(e^{(1-\alpha)\frac{F}{RT}\eta} - e^{-\alpha\frac{F}{RT}\eta} \right) \quad (2)$$

The two terms in the right hand side of eq 2 are shown as dashed lines in figure 2k. From a Tafel plot of η against log(*i*), extrapolating the current measured at high overpotential down to η=0 gives the exchange current i_0. Another measurement of the surface's activity is the "onset overpotential" defined as the overpotential above which the current exceeds an arbitrarily chosen threshold (often 10 mA/cm^2 for OER and HER[74,75]). The exchange current and the onset potential (of e.g. catalytic oxidation) are related to one another[75]:

$$\eta_{\text{onset}} = \frac{RT}{(1-\alpha)F} \log\left(\frac{i_{\text{threshold}}}{i_0}\right) \quad (3)$$

The catalytic current may reach a plateau at very high overpotential, but this maximum current does not characterize the catalyst: it may result from a limitation of the current by the transport towards the catalytic surface of O_2 in the ORR or H_2 in the HOR, or the formations of bubbles of the product of the HER or OER[74]. In any case, this high overpotential region of the electrochemical signal embeds no information about the catalytic mechanism.

The voltammetric responses of *molecular* redox catalysts look very different (figures 2 i-j). The current changes in a sigmoidal manner with η, and the plateaus on either side may be independent of any limitation by the transport of substrate towards the electrode. For example, if a molecular

catalyst is attached to a rotating electrode[76] spun at a high rate, the limiting currents are proportional to the intrinsic turnover frequency of the catalyst (TOF_{max}) under these conditions[72]. The sigmoidal signal defines "catalytic potentials" (E_{cat} in figure 2i, not to be confused with the catalyst's redox potentials measured under non-turnover conditions), or "catalytic overpotentials" ($\eta_{cat} = E_{cat} - E_{eq}$), where the current is half of its plateau value[3,77]. Unlike onset potentials, catalytic potentials are not dependent on the arbitrary choice of a current threshold. The separation between the catalytic potentials of the oxidative and reductive catalytic waves (E_{cat}^{ox} and E_{cat}^{red}) measures the reversibility of the catalytic response: a large separation implies that there is no current over a large range of potential, which is characteristic of an irreversible response (figure 2i), whereas the oxidative and reductive waves merge if the response is reversible (figure 2j).

Therefore, in the case of electrocatalysts, the onset potential and the exchange current are related to one another (eq. 2), and they both characterize the overall activity of the surface, whereas in the case of molecular catalysts, the turnover rate (which defines the magnitude of the current) and the reversibility (the splitting of the oxidative and reductive waves) are independent figures of merit.

The above distinction between rate and reversibility has been discussed in the case of biological motors in terms of tradeoffs between rate (or flux, J) and energetic efficiency[53,58]. The latter is defined as the fraction of the input free energy ($\Delta\mu$) that is transformed in output work (Δw); the rest, $\Delta\mu$-Δw, is dissipated. Regarding kinesin for example, $\Delta\mu$ is the free energy of ATP hydrolysis, and Δw is the work that is produced by moving over a certain distance against a certain force (figure 3a). This defines the power of the device, $P=J\Delta w$, and the power output per unit input energy $F=J\Delta w/\Delta\mu=J\eta$ (here the symbol η is used for the efficiency). The power is often plotted against work or force (as in figure 3b)[78]. The idea is the same as in the evaluation of the performance of fuels cells, for example, whose power $P=Ui$ (U the voltage of the cell and i the current) is plotted against output voltage U (the latter is changed by varying the resistance of the outer electrical circuit) (figure 3c-d). Wagoner and Dill have emphasized that rate and efficiency are independent properties of the biological motors, and suggested that in each case, a particular combination of the two is optimized by evolution: ATP-synthase for example, would be more optimized for efficiency than for speed[53].

The mean-field kinetic modeling of bidirectional catalysts

Understanding the relation between the rate of a reaction and the rate constants of all the steps in the mechanism is only trivial when the reaction sequence is either a single bidirectional step or a series of unidirectional steps (in the former case, the ratio of the forward and backward rate constants equates the equilibrium constant; in the latter, the reciprocal rate is simply the sum of the reciprocal rate constants of the individual steps). If the mechanism is more complex, it is common to steer clear of complex rate equations by assuming that one step in the cycle is unidirectional or by focussing exclusively on the *thermodynamics* of the reaction pathway[79].

Electrocatalysis

For unidirectional chemical reactions, the turnover frequency (TOF) depends on the "energy span", defined as the difference between the point of highest energy and that of lowest energy along the energy profile[80,81]; its evaluation requires the knowledge of the energy barriers. Since the latter are difficult to calculate, many DFT investigations of surface reaction mechanisms consider only the energies of the intermediates. The latter determine the complete energy profile only if the energy barriers $\Delta G^{\neq}$ are proportional to the free energy ΔG of the corresponding steps[79,82] (this relation between the two is known as the Bronsted-Evans-Polanyi linear scaling relationship). However, linear scaling is only expected when all steps in the catalytic cycle have a similar nature and transition state[83–85]. Different classes of reactions should give different linear relationships[85], and in the context of molecular catalysis there are many examples of fast endergonic steps (e.g. intramolecular ET in

multicentered enzymes[86,87]) and slow thermoneutral steps (see below the discussion of the $[Pt(depe)_2]^{2+}$ molecular catalyst of CO_2/formate conversion[39]).

A strong and common assumption in the qualitative kinetic modelling of electrocatalysis is to consider the catalytic cycle as a series of *redox* steps, each consisting of one electron transfer (ET) that is strictly coupled to chemical reactions such as reactants adsorption/desorption, (de)protonation and/or bond breaking or formation[88,89]. The forward and backward rate constants of each step "*i*" are typically assumed to change with the electrode potential *E* as predicted by Butler-Volmer theory[74,76,88,89]:

$$k_i^{\mathrm{ox}} = k_i^0 \exp\left(\frac{(1-\alpha_i)F}{RT}(E - E_i^0)\right) \quad (4a)$$

$$k_i^{\mathrm{red}} = k_i^0 \exp\left(\frac{-\alpha_i F}{RT}(E - E_i^0)\right) \quad (4b)$$

where the transfer coefficient α is related to the catalytic bias of the surface: indeed a value of α close to 0 or 1 results in the catalytic current being more intense in the oxidative or reductive direction (respectively)[74]. E^0_i is the thermodynamic reduction potential of step i, *F* is the Faraday constant, *R* the gas constant, *T* the temperature.

The consequence of the mechanistic assumption that all steps in the catalytic cycle involve ET is that the ΔGs of all steps become more negative as the overpotential increases, and the current increases exponentially and perpetually as the overpotential increases (eq. 2 and figure 2k)[75].

The additional assumption that for the reaction to occur, all elementary reaction steps have to be downhill in terms of free energy[90], justifies the common idea that the catalytic current can only flow when the overpotential exceeds a certain "thermodynamic overpotential" above which the least favorable *redox* step (the so-called "potential-determining step") becomes exergonic. Although this thermodynamic overpotential cannot be compared to any experimental quantity[75,91], this simple reasoning has proven very useful for screening catalysts. It also explains the large overpotential required for fast OER on oxide and metal surfaces : the difference between the energies of the intermediates "HO*" and "HOO*" (the asterisk indicates an adsorbate) is large under equilibrium conditions and similar on many different surfaces; it defines a universal lower limit for the thermodynamic overpotential of around 0.3 V, above which all steps are downhill[79,91,92].

Although the above reasoning has been very fruitful in the case of surface catalysts, it is impossible to endorse the claim that catalysis should occur only if all steps in the catalytic cycle are downhill. The TOF of a catalyst depends in a complex manner on the individual rate constants of many of the steps in the catalytic cycle, and the penalty that results from an uphill step can be mitigated by kinetics effects and/or downhill follow-up steps[3].

Molecular catalysis

The above assumption of strict coupling between ET and bond breaking/formation was given justification by DFT calculations in the case of the HER reaction on Pt[79], but some reactions on other surfaces involve decoupled proton and electron transfers[75,93].

In contrast, the kinetic modelling of the catalytic cycle of molecular redox catalysts *always* involves a sequence of redox and non-redox steps (referred to as "E" and "C" steps)[70]. The mechanism can be described by the sequence of redox and chemical (non-redox) steps, and named accordingly. For example the mechanism in fig 1c would be called EECC. That a mechanism includes redox steps (whose rates depend on electrode potential as in eqs 4) and non-redox steps (whose rates are independent of *E*) gives a typical sigmoidal shape to the corresponding current/potential response

(figure 2ij). At very large overpotential, the interfacial ET steps become very fast, and the chemical steps control the overall rate and define the values of the plateau currents. The free energy of the chemical steps in the catalytic cycle do not depend on electrode potential, and should not be used to calculate a "thermodynamic overpotential". There is no obligation that every chemical step should be thermoneutral for the catalyst to be bidirectional[3], but since all chemical steps are slower than 10^{12} s^{-1} (typical vibrational frequency), observing significant turnover frequencies (e.g. > $1s^{-1}$) in both directions of an ordered cycle implies that every equilibrium constant along the reaction pathway should be lower than 10^{12} (16 kcal/mol).

A major obstacle to using kinetics to interpret the electrochemical response of bidirectional redox molecular catalysts and to elucidate the kinetic determinants of reversibility is that the analytical kinetic models of *bidirectional* molecular catalysis are incredibly scarce. Indeed, a very usual simplification in molecular catalysis is to consider that the reaction is unidirectional, either because at least one step is unidirectional[94] or because the overall reaction is very exergonic[80,81]. As an example, Savéant and Costentin do not discuss any bidirectional catalytic cycle in their reference book on molecular electrochemistry[70]. Assuming that the catalytic cycle is unidirectional makes it impossible to connect the kinetic parameters of the model to the thermodynamics of the reaction (equilibrium constant, equilibrium potential etc.): a unidirectional step has an infinitely negative free energy, so a cycle that includes a unidirectional step theoretically proceeds forwards irrespective of the actual thermodynamic driving force. As a consequence, in kinetic models of unidirectional redox catalysis, the overpotential is not defined in reference to the equilibrium potential (like we do), but in reference to the redox potential of the catalyst; defined as such, the overpotential is not proportional to the free energy of the catalyzed reaction[95]. Using kinetic models in which all steps are bidirectional is therefore an absolute requirement if the goal is to discuss catalytic reversibility.

Only a handful of papers have reported *analytical* kinetic models of bidirectional, redox, molecular catalysis, most often for extremely simple kinetic schemes. Kano *et al* wrote a model of mediated electron transfer (MET) to a diffusing catalyst under conditions of semi-infinite diffusion[96]. Armstrong *et al* described the case of a bidirectional catalyst supported onto an electrode (figure 2f) and undergoing direct electron transfer (DET)[97]. Savéant recently described the situation of DET to a diffusing catalyst (figure 2d)[98]. We also recently studied the MET case, but under conditions of a very thin film (figure 2g), and taking explicitly into account the competition between mediated ET and catalytic turnover[99].

All of the above models consider a single redox transition of the catalyst, and one or more chemical steps whose rates are independent of the electrode potential. They all predict that, on condition that interfacial electron transfer is fast, the catalytic current/potential response is simply a "one-electron sigmoid",

$$i = \frac{i_{\mathrm{lim}}^{\mathrm{ox}} \exp^{F(E-E_{\mathrm{cat}}^{n=1})/RT} - i_{\mathrm{lim}}^{\mathrm{red}}}{1+\exp^{F(E-E_{\mathrm{cat}}^{n=1})/RT}} \quad (5)$$

were $i_{\mathrm{lim}}^{\mathrm{ox}}$ and $i_{\mathrm{lim}}^{\mathrm{red}}$ are the two plateau currents, and $E_{\mathrm{cat}}^{n=1}$ is *the* catalytic potential that defines the mid-point potential of this sigmoid.

According to these one-electron models of multi-electron catalysis, a bidirectional catalyst undergoing fast ET with an electrode can only function reversibly. Catalytic irreversibility can only result from slow interfacial ET, not considered in eq 5[4,5,98]. (In this discussion, like in the rest of the paper, the term "reversible" refers to the catalytic property, not to the rate of interfacial electron transfer, see Box 1.)

However, many reactions of interest involve more than one electron (two for the HER and HOR, four for the OER and ORR) and the above conclusion from one-electron models is proven wrong by more

realistic models that consider the *two* redox transitions of the active site[3,100]. Catalytic irreversibility may indeed occur even in the limit of Nernstian interfacial ET if, for example, the half-reduced form of the active site is stable over a large range of potential. In that case, the catalytic oxidative and reductive cycles are triggered by the formations of the fully oxidized and fully reduced form of the active site, respectively, which occur at different potentials. In the intermediate potential range, there is no activity: catalysis is irreversible. In *unidirectional* one-electron models of multi-electron reactions, considering a unique one-electron transition of the catalyst makes sense because the other redox processes are fast in the range of potential where catalysis is observed[70,101], but this assumption fails if one attempts to model the oxidative and reductive response of a bidirectional catalyst over a large range of potential. Thus, the "one-electron models'' do not have the minimal complexity that is required to discuss the determinants of catalytic reversibility in the case of multi-electron reactions.

We have recently discussed the analytical current equations for various bidirectional two-electron kinetic schemes, which can be used to interpret the DET voltammetry of supported[72,100] or diffusing[3,100] redox catalysts of two-electron reactions. In both cases, under conditions of steady-state and assuming fast interfacial electron transfer, all ordered mechanisms that include two redox steps and an unspecified number of chemical steps give the same rate equation:

$$i = \frac{i_{\mathrm{lim}}^{\mathrm{ox}}\ \exp^{F(E-E_{\mathrm{cat}}^{\mathrm{ox}})/RT}\ \exp^{F(E-E_{\mathrm{cat}}^{\mathrm{red}})/RT} - i_{\mathrm{lim}}^{\mathrm{red}}}{1+\exp^{F(E-E_{\mathrm{cat}}^{\mathrm{red}})/RT}(1+\exp^{F(E-E_{\mathrm{cat}}^{\mathrm{ox}})/RT})} \quad (6)$$

The parameters in eq 6 are defined in figure 2i: $i_{\mathrm{lim}}^{\mathrm{ox}}$ and $i_{\mathrm{lim}}^{\mathrm{red}}$ are the two plateau currents, the ratio of which measures the catalytic bias; $E_{\mathrm{cat}}^{\mathrm{ox}}$ and $E_{\mathrm{cat}}^{\mathrm{red}}$ are the two catalytic potentials, which may be distinct from the redox potentials of the catalyst measured under non-turnover conditions[3], and whose difference measures the catalytic reversibility (the more positive the difference $E_{\mathrm{cat}}^{\mathrm{ox}} - E_{\mathrm{cat}}^{\mathrm{red}}$ the less reversible the response). Equation 6 is the same for all two-electron ordered mechanisms (irrespective of the order of the steps in the catalytic cycle), but the right mechanism may be identified by comparing the catalytic and non-catalytic responses, or by examining how the waveform depends on the substrate and product concentrations[3].

The thermodynamic constraint that i=0 when the electrode potential (E) equates the Nernst potential of the substrate/product couple (E_{eq}) imposes the following relation:

$$\frac{i_{\mathrm{lim}}^{\mathrm{ox}}}{i_{\mathrm{lim}}^{\mathrm{red}}} = \exp\left[\frac{2F}{RT}\left(\frac{E_{\mathrm{cat}}^{\mathrm{ox}}+E_{\mathrm{cat}}^{\mathrm{red}}}{2} - E_{\mathrm{eq}}\right)\right] \quad (7)$$

which is the Haldane equation for an ordered, two-electron, multi-step catalytic mechanism. The experimental observation that eq 6 or 7 are valid in a particular case proves that the mechanism is ordered (as opposed to branched)[3].

Considering that all steps in the catalytic cycle are bidirectional led to unexpected theoretical findings.

For example, regarding a catalyst that diffuses towards an electrode and operates according to an ordered mechanism, the famous relation i_{lim}=nFAC(TOF$_{\mathrm{max}}$ D)$^{1/2}$ between the plateau current and the square root of turnover frequency[102] is wrong for all bidirectional mechanisms (compare the expressions of "TOF$_{\mathrm{max}}$" and "i_{lim}" in Table 1 of ref [3]). This is because i_{lim} depends on the concentration profile of the catalyst in the solution near the electrode, established by the mutual compensation of the diffusion of the catalyst and its transformation in solution, but the later depends on the rate constants of the chemical steps in the forward *and* backward directions of the reaction, irrespective of the electrode potential. All things being equal, increasing the backward rate constants decreases

the size of the reaction-diffusion layer near the electrode where catalysis occurs, and therefore decreases the forward current.

Moreover, if the two-electron catalytic cycle includes more than one bidirectional chemical step, then the two catalytic potentials in eq 7 necessarily depart from the reduction potentials of the catalysts measured in the absence of substrate[3]. This forbids using the popular "foot of the wave analysis"[103,104], which assumes that the catalytic sigmoidal wave is centered on the potential of the catalyst measured under non-catalytic conditions.

It is difficult to bound the errors made when one uses unidirectional models to interpret bidirectional electrochemical voltammograms. If the mechanism is simply EEC and the current is of the same order of magnitude in the two directions, estimating the turnover frequency from the limiting current using the relation i_{lim}=nFAC(TOF$_{max}$ D)$^{1/2}$, which is only valid for unidirectional catalysis, underestimates the TOF by only a factor of 2 (compare eqs 1 and 3 in Table 1 of ref. [3]), irrespective of whether the signal is reversible or irreversible; if the ratio of TOF max is 1:10, then the estimation of the TOF in the slowest direction (and the estimation of the bias) is wrong by a factor of 10. But for more complex and realistic mechanisms, there is no guarantee that the error should be small. Regarding the use of the foot of the wave analysis, each 60 mV difference between the true catalytic potential and the potential measured in the absence of catalysis results in a ten fold error on the extrapolated limiting current, and except for the simplest EC or EEC catalytic mechanisms, a difference between the catalytic and non catalytic potentials is always expected if the chemical steps are bidirectional[3].

Biological motors

The kinetics of molecular motors has also been described using ordered mechanisms and by examining the system in terms of a basic free energy landscape that is modified upon changing either the input free energy or the force (load) that opposes the work that is produced[9,105,106].

The formulation of the problem by Sivak *et al* brings out the analogy with the modelling of electrochemical systems: for each step *i* in the catalytic cycle, the ratio of the forward and backward rate constants depends on the free energy ω_i dissipated in that step,

$$\frac{k_i^f}{k_i^b} = \exp\left(\frac{\omega_i}{RT}\right) \quad (8)$$

and a splitting (or load-distribution) factor δ_i defines how each of the two rate constants vary with the free energy dissipation, and whether the transition state is close to the rear or front state

$$k_i^f = k_i^0 \exp\left(\frac{\delta_i \omega_i}{RT}\right) \quad (9a)$$

$$k_i^b = k_i^0 \exp\left(\frac{-(1-\delta_i)\omega_i}{RT}\right) \quad (9b)$$

The value of δ_i is related to the mechanism by which the consumption of free energy in this particular step produces *directed* molecular machine operation[9,29], just like the transfer coefficient α in eqs 4 may impose a directionality to certain ET steps in the cycle of a redox catalyst. Since equations 4 and 9 are analogous, the flux and current equations obtained with models of molecular motors and surface catalysts are similar (compare eq 20 in ref [9] for the two-stage model of motor and the current equation for a catalytic cycle consisting of just two redox steps, e.g. in ref [88]).

The flux equations for two and three-stage models show that maximal rate is achieved when more free energy (larger ω_i) is dissipated by steps that are slower at equilibrium (small k_i^0), hence the

maximal rate is not obtained with an equal change in free energy across all steps[107,108]; this conclusion is also true, but probably overlooked, in the case of multi-step chemical reactions.

In other formulations[53,58,109,110], the driving force ω is explicitly considered as the difference between the input chemical free energy of e.g. ATP hydrolysis, Δμ, and the work that is produced, Δw. In ref [110], a parameter δ dictates how much Δw affects the forward and backward rates of each step. Assuming a certain four-steps catalytic cycle, which includes in a specific order steps that are (i) independent of Δμ and Δw, (ii) dependent of Δμ (e.g. $k_i^f=k_i^0 \exp[\Delta\mu/RT]$, $k_i^b=k_i^0$), (iii) dependent of Δw (e.g. $k_i^f = k_i^0 \exp[-\delta\Delta w/RT]$, $k_i^b = k_i^0 \exp[(1-\delta)\Delta w/RT]$), it is possible to calculate how the response depends on δ by examining the relations between rate *J*, work Δw, and power ($J\times\Delta w$)[110]. In the two-step model of ref [58], only one step depends on Δw, and a parameter λ defines how Δμ is expanded in each of the 2 steps. Therein the authors focus on the relation between rate and efficiency ($\eta=\Delta w/\Delta\mu$)[58]; this is directly related to our definition of "reversibility" since the free energy that is dissipated to drive the motor is $\Delta\mu(1-\eta)$ (fig 1o).

The approach that was recently used to model the kinetics of artificial chemically-driven motors is distinct: it considers a branched mechanism and the possibility of uncoupling[111,112] (as indeed occurs in the kinesin mechanism in figure 1f). This kinetic model explains the direction of motion, but the work is not explicitly defined and the efficiency is therefore not discussed[111,112].

The million dollar question of the determinants of catalytic reversibility

The most popular strategy in electrocatalyst screening and design is to quest for thermoneutral binding of the molecule to be transformed. This reasoning is based on the Sabatier principle, according to which the most active catalyst binds its substrate neither too weakly nor too strongly[113], thus optimizing the tradeoff between rate and catalyst poisoning. If this binding energy is indeed a good thermodynamic "descriptor", a "volcano plot" of activity against binding energy should show a single maximum[89,114,115].

This strategy has echoed in the molecular catalysis field, but with no proper discussion of whether or why thermoneutral binding should make the catalyst fast, or bidirectional, or reversible, or all of this at once. But the point has also been made that the Sabatier principle, and its illustration in volcano plots, is not the full picture.

Costentin and Savéant have strongly advocated against considerations based on volcano plots for the understanding and design of *unidirectional* molecular catalysts[116,117]. Their point was that the properties of these catalysts should be characterized in terms of catalytic potentials *and* maximal turnover frequencies (reached at high overpotential), rather than just the TOF obtained at a certain potential. Regarding *bidirectional* molecular catalysts, we add that even the simplest catalytic responses should be defined by not two but three independent figures of merit: rate (e.g. the TOFmax under oxidizing conditions), bias (the ratio of the oxidative and reductive TOFmax) and reversibility (the separation between the oxidative and reductive waves, figure 2i). There is no obvious reason why rate, bias and reversibility should obey the same design principles, and in our investigation of the multistep catalytic cycles of two-electron transformations, we demonstrated that neither bidirectionality nor reversibility requires that all steps in the catalytic cycle be thermoneutral[3].

An example of reversible catalyst design driven by the application of the Sabatier principle is the recent demonstration by Jenny Y. Yang that a $[Pt(depe)_2]^{2+}$ (depe=1,2-bis(diethylphosphino)ethane) complex reversibly converts CO_2/HCO_2^- in acetonitrile (figure 1c)[118]. Turnover is very slow, because the Pt hydride intermediate reacts with CO_2 (1 atm) with a pseudo-1st order rate constant of about 1 $hour^{-1}$ at 298K (ref [119]). However, the energy landscape of this catalytic cycle is described as ideally flat[118]; in particular the hydricities[120,121] of $[HPt(depe)_2]$ and HCO_2^- are equal, which ensures

thermoneutral hydride transfer from $[HPt(depe)_2]^+$ to CO_2. According to Yang et al, this makes the catalyst function reversibly[118].

Using the conclusions from ref [3], we can emphasize two other reasons why this $[Pt(depe)_2]^{2+}$ may function reversibly and equally fast in both directions.

First, the reduction from $[Pt(depe)_2]^{2+}$ to $[Pt(depe)_2]^0$ is a cooperative two-electron process[122]. Should the half-reduced state $[Pt(depe)_2]^+$ be stable over a large range of potential and the same mechanism be operational, then CO_2 reduction would occur at a lower potential than formate oxidation, and catalysis would be irreversible. The cooperative nature of the 2+/0 redox step implies that the 1+, half reduced catalyst is a high energy intermediate, which contradicts the alleged requirement for a flat energy landscape. However, the participation of a high energy intermediate does not slow catalysis if the corresponding ET step is fast compared to turnover. The assumption that interfacial ET steps are Nernstian (as defined in Box 1) is common in the modeling of redox molecular catalysis[116], and certainly valid in the particular case of $[Pt(depe)_2]^{2+}$ (ref [3]).

Second, for a catalytic cycle that includes a cooperative two-electron redox step followed by one or two chemical steps, the conclusions in ref [3] imply that the average value of the two catalytic potentials equates the potential of the average two-electron reduction potential of the catalyst, and using eq. 7 we conclude that the difference between the later and the equilibrium potential of the substrate/product couple defines the catalytic bias. That the potential of the $[Pt(depe)_2]^{2+/0}$ catalyst is very close to the potential of the CO_2/formate couple[118] therefore ensures that the oxidative and reductive catalytic currents are nearly equal.

Therefore, any further attempt to increase the TOF of this Pt catalyst by accelerating the reaction of the metal hydride with CO_2 will have to preserve these two conditions.

In the redox enzymes field, *E. coli* fumarate reductase (QFR) is another example of a mechanism that involves two successive one-electron transfers to/from the active site flavin, followed by chemical steps (hydride transfer between the flavin and the substrate, and proton transfer from an arginine residue[123]). It is an "EECC" mechanisms[3] (noting here that each redox step is coupled to fast substrate and product binding and release, which affect its potential). The two-electron potential of the flavin is slightly lower than the potential of the succinate/fumarate couple, resulting in a bias towards fumarate reduction. Like $[Pt(depe)_2]^{2+/0}$, the redox transformation of the flavin is cooperative, which makes catalysis reversible (as observed in fig 1 of ref [63]). In contrast, the homologous enzyme fcc_3 from *Shewanella oneidensis* catalyses only fumarate reduction, consistent with the two-electron potential of the flavin in this enzyme being lower than in *E. coli* QFR[124].

The DuBois catalysts, whose generic structure is shown in Figure 1d, have attracted much attention for their performance in terms of rate of HOR/HER and reversibility, which proved to be very dependent on the nature of the R and R' substituents. Tradeoffs between rate and bidirectionality have been observed: for example the bidirectional complexes[40,42] are orders of magnitude slower than the R=R'=phenyl catalyst, although the latter works only in the direction of proton reduction and at the price of a large overpotential [125,126]. It behaves reversibly in acidic water when it is modified and grafted onto nanotubes (figure 2e)[127], for reasons that are not entirely clear.

A major step forward was the design of the R=Phe, $R'=CH_2CH_2OCH_3$ complex: based on NMR results, the free energy of reaction of this Ni(II) complex with H_2 is around 0.9 kcal/mol [39] (this reaction involves the initial binding of H_2, which is uphill by approximately 7-10 kcal/mol, followed by downhill H_2 heterolytic splitting and intramolecular proton transfer[43,128]). This small value is very favorable according to the Sabatier principle and indeed, the complex oxidises and produces H_2 in acetonitrile (bidirectionally but irreversibly and with a strong bias)[39]. However, the proton redistribution that follows H_2 splitting in that "H_2 binding" reaction[39] produces various isomers that are not part of the catalytic cycle; this raises questions regarding why the empirical relation between H_2 binding energy

and catalytic bias or reversibility is actually observed. Related complexes were later found to exhibit even better performance: bidirectionality in water (R=cyclohexyl, R'=glycine)[12], *reversibility* in acidic water at 348 K (R=cyclohexyl, R'=arginine)[40], reversibility at room temperature in acidic methanol (R=cyclohexyl, R'=phenyl) and in methanol or water (R=cyclohexyl, R'=tyrosine, phenyl or tyramine)[42]. The free energy could not be measured in each case, but we note that the reaction of H_2 with the R=Cy R'=Arg complex is significantly exergonic at 348 K, despite catalysis being reversible at that temperature[40].

The reason some of the DuBois catalysts behave reversibly must still be clarified, but it probably involves a number of contributing factor in addition to (or instead of) the thermoneutrality of the reaction with H_2 : the stabilization of certain isomers, the kinetics of intramolecular proton transfer to/from the side chains of the complex[42], the affinity for protons (not just H_2) and the potentials of the various redox transitions of the active site.

A difficulty in the assessment of the voltammetry of the bidirectional DuBois catalysts is that in some of the experimental cases that we have examined, equation 7 is not obeyed[3], which shows that the mechanism is branched, as is common in inorganic redox catalysis[129–136]. This is a major issue because there is only one analytical model (from our group) of bidirectional, redox catalysis for a mechanism with parallel pathways; it was aimed at discussing the effect of intramolecular ET through an internal relay on the voltammetry of a supported enzyme[100]. From our investigations of kinetic models of *unidirectional,* branched mechanisms[137,138], we can be certain that very complex waveforms can be expected from the corresponding bidirectional models. The latter will not be easily extended to the cases of diffusing catalysts, and simulations such as those in refs [139,140] will probably be more useful in the short term.

Based on the conclusions in ref [3] and contrary to common assumption, we can however say for sure that *irreversible* catalysis does *not* imply that the mechanism is branched, or that forward and backward reactions follow distinct pathways: irreversible voltammograms can be obtained with ordered models under certain conditions. Nor does a branched mechanism imply an irreversible response; on the contrary, we expect more degrees of freedom and a wider variety of catalytic responses and properties allowed by branched mechanisms. A challenge will be to explore these situations theoretically, to become able to make full use of electrochemical methods to explain the voltammetry of DuBois and other bidirectional catalysts as they are developed in the future, and to clarify what are the kinetic determinants of reversibility in this class of catalysts.

In the case of bioelectrocatalysis, the design of reversible systems should also consider the charge transfer pathway from the active site of the enzyme to the electrode. A common idea is that an irreversible response is expected for redox enzymes under conditions of mediated electron transfer, because some energy loss is allegedly required to produce the significant driving force that allows fast ET[141,142]. Indeed, a large difference between the redox potentials of the mediator and of the enzyme was needed to obtain large current densities when unidirectional enzymes were immobilized in redox-active films (figure 2g)[143,144], and when this configuration was used with formate dehydrogenases or hydrogenases, the intrinsic reversibility of these enzymes was lost[145,146–151].

However, reversible catalytic responses under conditions of mediated ET with 4,4'-methylviologen have actually been observed with hydrogenases[147,152,153], and we recently showed that the catalytic reversibility of FeFe hydrogenase is preserved when this enzyme is embedded into a film of a specially designed low potential redox-active hydrogel based on 2,2´-methylviologen (figure 2n)[99]. The catalytic wave remains centered in the potential of the viologen, which results from intermolecular ET between the artificial mediator and the catalyst being slower than catalysis itself, but this appears not to prevent catalytic reversibility. This is reminiscent of the natural electron transfer pathway of *Megasphaera elsdenii* FeFe hydrogenase: this enzyme reversibly oxidizes and

produces H_2 despite intramolecular ET (between the iron-sulfur clusters acting as electronic relays and the active site) being rate-determining in both directions of the reaction[15].

Understanding the effect of the potential mismatch between the electron mediator and the enzyme on the catalytic bias, the TOF and the catalytic potentials will be essential for making high power biofuel cells, with large current densities close to the equilibrium potential (fig 3d).

Conclusion

Catalytic reversibility is a very desirable property, which appears to be common in Nature, but has been difficult to characterize experimentally (except in electrochemistry) and to engineer in molecular catalysts.

We have paralleled the discussions regarding the determinants of catalytic directionality and reversibility that are present in electrocatalysis, molecular catalysis, and the studies of biological motors. It appears that the concepts coincide, although the vocabulary is distinct. This is a source of confusion that will have to be removed in the future.

For example, reversibility has been claimed in the field of energy conversion/storage (e.g de/hydrogenation[154–158]), but this was actually with the meaning of chemical reversibility (bidirectionality). We hope that lessons learned in reversible catalysis (as we defined it here) in the context of electrocatalysis and molecular machines will prove highly valuable for improving the energy efficiency in classical chemical catalysis.

We also believe that an important step forward is to acknowledge that rate, directionality and reversibility are distinct figures of merit, which may obey different design principles. Thinking in terms of Sabatier principle, thermodynamic descriptors or volcano plots will not be enough, and we should aim for developing analytical kinetic models that will be required to understand the determinants of reversibility.

References

(1) Nicholls, D. G.; Ferguson, S. J. Bioenergetics; Academic Press, 2013.
(2) De Luna, P.; Hahn, C.; Higgins, D.; Jaffer, S. A.; Jaramillo, T. F.; Sargent, E. H. What Would It Take for Renewably Powered Electrosynthesis to Displace Petrochemical Processes? Science 2019, 364 (6438). doi: 10.1126/science.aav3506
(3) Fourmond, V.; Wiedner, E. S.; Shaw, W. J.; Léger, C. Understanding and Design of Bidirectional and Reversible Catalysts of Multielectron, Multistep Reactions. J. Am. Chem. Soc. 2019, 141 (28), 11269–11285. doi: 10.1021/jacs.9b04854
(4) Dutta, A.; Appel, A. M.; Shaw, W. J. Designing Electrochemically Reversible H2 Oxidation and Production Catalysts. Nature Reviews Chemistry 2018, 2 (9), 244–252. doi: 10.1038/s41570-018-0032-8
(5) Armstrong, F. A.; Hirst, J. Reversibility and Efficiency in Electrocatalytic Energy Conversion and Lessons from Enzymes. Proc. Natl. Acad. Sci. U. S. A. 2011, 108 (34), 14049–14054. doi: 10.1073/pnas.1103697108
(6) Domnik, L.; Merrouch, M.; Goetzl, S.; Jeoung, J.-H.; Léger, C.; Dementin, S.; Fourmond, V.; Dobbek, H. CODH-IV: A High-Efficiency CO-Scavenging CO Dehydrogenase with Resistance to O2. Angew. Chem. Int. Ed Engl. 2017, 56 (48), 15466–15469. doi: 10.1002/anie.201709261
(7) Alberty, R. A.; Hammes, G. G. Application of the Theory of Diffusion-Controlled Reactions to Enzyme Kinetics. J. Phys. Chem. 1958, 62 (2), 154–159. doi: 10.1021/j150560a005
(8) Bar-Even, A.; Noor, E.; Savir, Y.; Liebermeister, W.; Davidi, D.; Tawfik, D. S.; Milo, R. The Moderately Efficient Enzyme: Evolutionary and Physicochemical Trends Shaping Enzyme Parameters. Biochemistry 2011, 50 (21), 4402–4410. doi: 10.1021/bi2002289
(9) Brown, A. I.; Sivak, D. A. Theory of Nonequilibrium Free Energy Transduction by Molecular Machines. Chem. Rev. 2020, 120 (1), 434–459. doi: 10.1021/acs.chemrev.9b00254
(10) Jencks, W. P. Catalysis in Chemistry and Enzymology; Courier Corporation, 1987.

(11) Lampret, O.; Duan, J.; Hofmann, E.; Winkler, M.; Armstrong, F. A.; Happe, T. The Roles of Long-Range Proton-Coupled Electron Transfer in the Directionality and Efficiency of [FeFe]-Hydrogenases. Proc. Natl. Acad. Sci. U. S. A. 2020, 117 (34), 20520–20529. doi: 10.1073/pnas.2007090117
(12) Dutta, A.; Lense, S.; Hou, J.; Engelhard, M. H.; Roberts, J. A. S.; Shaw, W. J. Minimal Proton Channel Enables H2 Oxidation and Production with a Water-Soluble Nickel-Based Catalyst. J. Am. Chem. Soc. 2013, 135 (49), 18490–18496. doi: 10.1021/ja407826d
(13) Léger, C.; Bertrand, P. Direct Electrochemistry of Redox Enzymes as a Tool for Mechanistic Studies. Chem. Rev. 2008, 108 (7), 2379–2438. doi: 10.1021/cr0680742
(14) Abou Hamdan, A.; Dementin, S.; Liebgott, P.-P.; Gutierrez-Sanz, O.; Richaud, P.; De Lacey, A. L.; Rousset, M.; Bertrand, P.; Cournac, L.; Léger, C. Understanding and Tuning the Catalytic Bias of Hydrogenase. J. Am. Chem. Soc. 2012, 134 (20), 8368–8371. doi: 10.1021/ja301802r
(15) Caserta, G.; Papini, C.; Adamska-Venkatesh, A.; Pecqueur, L.; Sommer, C.; Reijerse, E.; Lubitz, W.; Gauquelin, C.; Meynial-Salles, I.; Pramanik, D.; Artero, V.; Atta, M.; Del Barrio, M.; Faivre, B.; Fourmond, V.; Léger, C.; Fontecave, M. Engineering an [FeFe]-Hydrogenase: Do Accessory Clusters Influence O2 Resistance and Catalytic Bias? J. Am. Chem. Soc. 2018, 140 (16), 5516–5526. doi: 10.1021/jacs.8b01689
(16) McIntosh, C. L.; Germer, F.; Schulz, R.; Appel, J.; Jones, A. K. The [NiFe]-Hydrogenase of the Cyanobacterium Synechocystis Sp. PCC 6803 Works Bidirectionally with a Bias to H2 Production. J. Am. Chem. Soc. 2011, 133 (29), 11308–11319. doi: 10.1021/ja203376y
(17) Lampret, O.; Adamska-Venkatesh, A.; Konegger, H.; Wittkamp, F.; Apfel, U.-P.; Reijerse, E. J.; Lubitz, W.; Rüdiger, O.; Happe, T.; Winkler, M. Interplay between CN Ligands and the Secondary Coordination Sphere of the H-Cluster in [FeFe]-Hydrogenases. J. Am. Chem. Soc. 2017, 139 (50), 18222–18230. doi: 10.1021/jacs.7b08735
(18) Adamson, H.; Robinson, M.; Wright, J. J.; Flanagan, L. A.; Walton, J.; Elton, D.; Gavaghan, D. J.; Bond, A. M.; Roessler, M. M.; Parkin, A. Retuning the Catalytic Bias and Overpotential of a [NiFe]-Hydrogenase via a Single Amino Acid Exchange at the Electron Entry/Exit Site. J. Am. Chem. Soc. 2017, 139 (31), 10677–10686. doi: 10.1021/jacs.7b03611
(19) Rodríguez-Maciá, P.; Kertess, L.; Burnik, J.; Birrell, J. A.; Hofmann, E.; Lubitz, W.; Happe, T.; Rüdiger, O. His-Ligation to the [4Fe-4S] Sub-Cluster Tunes the Catalytic Bias of [FeFe] Hydrogenase. J. Am. Chem. Soc. 2019, 141 (1), 472–481. doi: 10.1021/jacs.8b11149
(20) Therien, J. B.; Artz, J. H.; Poudel, S.; Hamilton, T. L.; Liu, Z.; Noone, S. M.; Adams, M. W. W.; King, P. W.; Bryant, D. A.; Boyd, E. S.; Peters, J. W. The Physiological Functions and Structural Determinants of Catalytic Bias in the [FeFe]-Hydrogenases CpI and CpII of Strain W5. Front. Microbiol. 2017, 8, 1305. doi: 10.3389/fmicb.2017.01305
(21) Kertess, L.; Adamska-Venkatesh, A.; Rodríguez-Maciá, P.; Rüdiger, O.; Lubitz, W.; Happe, T. Influence of the [4Fe-4S] Cluster Coordinating Cysteines on Active Site Maturation and Catalytic Properties of [FeFe]-Hydrogenase. Chem. Sci. 2017, 8 (12), 8127–8137. doi: 10.1039/c7sc03444j
(22) Mulder, D. W.; Peters, J. W.; Raugei, S. Catalytic Bias in Oxidation-Reduction Catalysis. Chem. Commun. 2021, 57 (6), 713–720. doi: 10.1039/d0cc07062a
(23) Cornish-Bowden, A. Fundamentals of Enzyme Kinetics (English Edition), 4th ed.; Wiley-Blackwell, 2013.
(24) Jencks, W. P. Binding Energy, Specificity, and Enzymic Catalysis: The Circe Effect. Adv. Enzymol. Relat. Areas Mol. Biol. 1975, 43, 219–410. doi: 10.1002/9780470122884.ch4
(25) Frydendal, R.; Paoli, E. A.; Knudsen, B. P.; Wickman, B.; Malacrida, P.; Stephens, I. E. L.; Chorkendorff, I. Benchmarking the Stability of Oxygen Evolution Reaction Catalysts: The Importance of Monitoring Mass Losses. CHEMELECTROCHEM 2014, 1 (12), 2075–2081. doi: 10.1002/celc.201402262
(26) Jaramillo, T. F.; Jørgensen, K. P.; Bonde, J.; Nielsen, J. H.; Horch, S.; Chorkendorff, I. Identification of Active Edge Sites for Electrochemical H2 Evolution from MoS2 Nanocatalysts. Science 2007, 317 (5834), 100–102. doi: 10.1126/science.1141483
(27) Carter, N. J.; Cross, R. A. Mechanics of the Kinesin Step. Nature 2005, 435 (7040), 308–312. doi: 10.1038/nature03528
(28) Clancy, B. E.; Behnke-Parks, W. M.; Andreasson, J. O. L.; Rosenfeld, S. S.; Block, S. M. A Universal Pathway for Kinesin Stepping. Nat. Struct. Mol. Biol. 2011, 18 (9), 1020–1027. doi: 10.1038/nsmb.2104
(29) Tsygankov, D.; Fisher, M. E. Mechanoenzymes under Superstall and Large Assisting Loads Reveal Structural Features. Proc. Natl. Acad. Sci. U. S. A. 2007, 104 (49), 19321–19326. doi: 10.1073/pnas.0709911104
(30) Skúlason, E.; Tripkovic, V.; Björketun, M. E.; Gudmundsdóttir, S.; Karlberg, G.; Rossmeisl, J.; Bligaard, T.; Jónsson, H.; Nørskov, J. K. Modeling the Electrochemical Hydrogen Oxidation and Evolution Reactions on

the Basis of Density Functional Theory Calculations. J. Phys. Chem. C 2010, 114 (42), 18182–18197. doi: 10.1021/jp1048887

(31) Damjanovic, A.; Dey, A.; Bockris, J. O. Kinetics of Oxygen Evolution and Dissolution on Platinum Electrodes. Electrochim. Acta 1966, 11 (7), 791–814. doi: 10.1016/0013-4686(66)87056-1

(32) Barrio, M.; Fourmond, V. Redox (In)activations of Metalloenzymes: A Protein Film Voltammetry Approach. ChemElectroChem 2019, 6 (19), 4949–4962. doi: 10.1002/celc.201901028

(33) Abou Hamdan, A.; Burlat, B.; Gutiérrez-Sanz, O.; Liebgott, P.-P.; Baffert, C.; De Lacey, A. L.; Rousset, M.; Guigliarelli, B.; Léger, C.; Dementin, S. O2-Independent Formation of the Inactive States of NiFe Hydrogenase. Nat. Chem. Biol. 2013, 9 (1), 15–17. doi: 10.1038/nchembio.1110

(34) Winkler, M.; Duan, J.; Rutz, A.; Felbek, C.; Scholtysek, L.; Lampret, O.; Jaenecke, J.; Apfel, U. P.; Gilardi, G.; Valetti, F.; Fourmond, V.; Hofmann, E.; Léger, C.; Happe, T. A Safety Cap Protects Hydrogenase from Oxygen Attack. Nat. Comm. 2021, 12, 756. doi: 10.1038/s41467-020-20861-2

(35) Artz, J. H.; Zadvornyy, O. A.; Mulder, D. W.; Keable, S. M.; Cohen, A. E.; Ratzloff, M. W.; Williams, S. G.; Ginovska, B.; Kumar, N.; Song, J.; McPhillips, S. E.; Davidson, C. M.; Lyubimov, A. Y.; Pence, N.; Schut, G. J.; Jones, A. K.; Soltis, S. M.; Adams, M. W. W.; Raugei, S.; King, P. W.; Peters, J. W. Tuning Catalytic Bias of Hydrogen Gas Producing Hydrogenases. J. Am. Chem. Soc. 2020, 142 (3), 1227–1235. doi: 10.1021/jacs.9b08756

(36) Jacq-Bailly, A.; Benvenuti, M.; Payne, N.; Kpebe, A.; Felbek, C.; Fourmond, V.; Léger, C.; Brugna, M.; Baffert, C. Electrochemical Characterization of a Complex FeFe Hydrogenase, the Electron-Bifurcating Hnd From Desulfovibrio Fructosovorans. Front Chem 2020, 8, 573305. doi: 10.3389/fchem.2020.573305.

(37) Segel, I. H. Enzyme Kinetics: Behavior and Analysis of Rapid Equilibrium and Steady-State Enzyme Systems; Wiley, 1975.

(38) Alberty, R. A. The Relationship between Michaelis Constants, Maximum Velocities and the Equilibrium Constant for an Enzyme-Catalyzed Reaction. J. Am. Chem. Soc. 1953, 75 (8), 1928–1932. https://dx.doi.org/10.1021/ja01104a045

(39) Smith, S. E.; Yang, J. Y.; DuBois, D. L.; Bullock, R. M. Reversible Electrocatalytic Production and Oxidation of Hydrogen at Low Overpotentials by a Functional Hydrogenase Mimic. Angew. Chem. Int. Ed Engl. 2012, 51 (13), 3152–3155. doi: 10.1002/anie.201108461.

(40) Dutta, A.; DuBois, D. L.; Roberts, J. A. S.; Shaw, W. J. Amino Acid Modified Ni Catalyst Exhibits Reversible H2 Oxidation/production over a Broad pH Range at Elevated Temperatures. Proc. Natl. Acad. Sci. U. S. A. 2014, 111 (46), 16286–16291. doi: 10.1073/pnas.1416381111

(41) Dutta, A.; Lense, S.; Roberts, J. A. S.; Helm, M. L.; Shaw, W. J. The Role of Solvent and the Outer Coordination Sphere on H2 Oxidation Using [Ni(PCy2NPyz2)2]2+ : The Role of Solvent and the Outer Coordination Sphere on H 2 Oxidation. Eur. J. Inorg. Chem. 2015, 2015 (31), 5218–5225. doi: 10.1002/ejic.201500732.

(42) Priyadarshani, N.; Dutta, A.; Ginovska, B.; Buchko, G. W.; O'Hagan, M.; Raugei, S.; Shaw, W. J. Achieving Reversible H2/H+ Interconversion at Room Temperature with Enzyme-Inspired Molecular Complexes: A Mechanistic Study. ACS Catal. 2016, 6 (9), 6037–6049. doi: 10.1021/acscatal.6b01433.

(43) Raugei, S.; Helm, M. L.; Hammes-Schiffer, S.; Appel, A. M.; O'Hagan, M.; Wiedner, E. S.; Bullock, R. M. Experimental and Computational Mechanistic Studies Guiding the Rational Design of Molecular Electrocatalysts for Production and Oxidation of Hydrogen. Inorg. Chem. 2016, 55 (2), 445–460. doi: 10.1021/acs.inorgchem.5b02262.

(44) Yang, J. Y.; Chen, S.; Dougherty, W. G.; Kassel, W. S.; Bullock, R. M.; DuBois, D. L.; Raugei, S.; Rousseau, R.; Dupuis, M.; Rakowski DuBois, M. Hydrogen Oxidation Catalysis by a Nickel Diphosphine Complex with Pendant Tert-Butyl Amines. Chem. Commun. 2010, 46 (45), 8618–8620. doi: 10.1039/c0cc03246h.

(45) Blackmond, D. G. "If Pigs Could Fly" Chemistry: A Tutorial on the Principle of Microscopic Reversibility. Angew. Chem. Int. Ed Engl. 2009, 48 (15), 2648–2654. https://dx.doi.org/10.1002/anie.200804566

(46) Pezzato, C.; Cheng, C.; Stoddart, J. F.; Astumian, R. D. Mastering the Non-Equilibrium Assembly and Operation of Molecular Machines. Chem. Soc. Rev. 2017, 46 (18), 5491–5507. doi: 10.1039/c7cs00068e.

(47) Fersht, A.; University Alan Fersht. Structure and Mechanism in Protein Science: A Guide to Enzyme Catalysis and Protein Folding; W. H. Freeman, 1999.

(48) Costentin, C. Proton-Coupled Electron Transfer Catalyst: Homogeneous Catalysis. Application to the Catalysis of Electrochemical Alcohol Oxidation in Water. ACS Catal. 2020, 10 (12), 6716–6725. doi: 10.1021/acscatal.0c01195.

(49) Horvath, S.; Fernandez, L. E.; Soudackov, A. V.; Hammes-Schiffer, S. Insights into Proton-Coupled Electron

Transfer Mechanisms of Electrocatalytic H2 Oxidation and Production. Proc. Natl. Acad. Sci. U. S. A. 2012, 109 (39), 15663–15668. doi: 10.1073/pnas.1118333109.
(50) Hyeon, C.; Klumpp, S.; Onuchic, J. N. Kinesin's Backsteps under Mechanical Load. Phys. Chem. Chem. Phys. 2009, 11 (24), 4899–4910. doi: 10.1039/b903536b.
(51) Ariga, T.; Tomishige, M.; Mizuno, D. Nonequilibrium Energetics of Molecular Motor Kinesin. Phys. Rev. Lett. 2018, 121 (21), 218101. doi: 10.1103/PhysRevLett.121.218101.
(52) Carter, N. J.; Cross, R. A. Kinesin's Moonwalk. Curr. Opin. Cell Biol. 2006, 18 (1), 61–67. doi: 10.1016/j.ceb.2005.12.009.
(53) Wagoner, J. A.; Dill, K. A. Opposing Pressures of Speed and Efficiency Guide the Evolution of Molecular Machines. Mol. Biol. Evol. 2019, 36 (12), 2813–2822. doi: 10.1093/molbev/msz190.
(54) Clark, E. L.; Bell, A. T. Chapter 3: Heterogeneous Electrochemical CO2 Reduction. In Carbon Dioxide Electrochemistry; Robert, M., Costentin, C., Daasbjerg, K., Eds.; RSC, 2020; pp 98–150. doi: 10.1039/9781788015844-00098.
(55) Piontek, S.; Junge Puring, K.; Siegmund, D.; Smialkowski, M.; Sinev, I.; Tetzlaff, D.; Roldan Cuenya, B.; Apfel, U.-P. Bio-Inspired Design: Bulk Iron-Nickel Sulfide Allows for Efficient Solvent-Dependent CO2 Reduction. Chem. Sci. 2019, 10 (4), 1075–1081. doi: 10.1039/c8sc03555e.
(56) Hoffman, B. M.; Lukoyanov, D.; Yang, Z.-Y.; Dean, D. R.; Seefeldt, L. C. Mechanism of Nitrogen Fixation by Nitrogenase: The next Stage. Chem. Rev. 2014, 114 (8), 4041–4062. doi: 10.1021/cr400641x.
(57) van Dijk, C.; Veeger, C. The Effects of pH and Redox Potential on the Hydrogen Production Activity of the Hydrogenase from Megasphaera Elsdenii. Eur. J. Biochem. 1981, 114 (2), 209–219. doi: 10.1111/j.1432-1033.1981.tb05138.x.
(58) Wagoner, J. A.; Dill, K. A. Mechanisms for Achieving High Speed and Efficiency in Biomolecular Machines. Proc. Natl. Acad. Sci. U. S. A. 2019, 116 (13), 5902–5907. doi: 10.1073/pnas.1812149116.
(59) Toyabe, S.; Watanabe-Nakayama, T.; Okamoto, T.; Kudo, S.; Muneyuki, E. Thermodynamic Efficiency and Mechanochemical Coupling of F1-ATPase. Proc. Natl. Acad. Sci. U. S. A. 2011, 108 (44), 17951–17956. doi: 10.1073/pnas.1106787108.
(60) Bianco, P.; Haladjian, J. Electrocatalytic Hydrogen-Evolution at the Pyrolytic Graphite Electrode in the Presence of Hydrogenase. J. Electrochem. Soc. 1992, 139 (9), 2428. doi: 10.1149/1.2221244.
(61) Butt, J. N.; Filipiak, M.; Hagen, W. R. Direct Electrochemistry of Megasphaera Elsdenii Iron Hydrogenase. Definition of the Enzyme's Catalytic Operating Potential and Quantitation of the Catalytic Behaviour over a Continuous Potential Range. Eur. J. Biochem. 1997, 245 (1), 116–122. doi: 10.1111/j.1432-1033.1997.00116.x.
(62) Pershad, H. R.; Duff, J. L.; Heering, H. A.; Duin, E. C.; Albracht, S. P.; Armstrong, F. A. Catalytic Electron Transport in Chromatium Vinosum [NiFe]-Hydrogenase: Application of Voltammetry in Detecting Redox-Active Centers and Establishing That Hydrogen Oxidation Is Very Fast Even at Potentials close to the Reversible H+/H2 Value. Biochemistry 1999, 38 (28), 8992–8999. doi: 10.1021/bi990108v.
(63) Léger, C.; Heffron, K.; Pershad, H. R.; Maklashina, E.; Luna-Chavez, C.; Cecchini, G.; Ackrell, B. A.; Armstrong, F. A. Enzyme Electrokinetics: Energetics of Succinate Oxidation by Fumarate Reductase and Succinate Dehydrogenase. Biochemistry 2001, 40 (37), 11234–11245. doi: 10.1021/bi010889b.
(64) Sucheta, A.; Ackrell, B. A.; Cochran, B.; Armstrong, F. A. Diode-like Behaviour of a Mitochondrial Electron-Transport Enzyme. Nature 1992, 356 (6367), 361–362. doi: 10.1038/356361a0.
(65) Parkin, A.; Seravalli, J.; Vincent, K. A.; Ragsdale, S. W.; Armstrong, F. A. Rapid and Efficient Electrocatalytic CO2/CO Interconversions by Carboxydothermus Hydrogenoformans CO Dehydrogenase I on an Electrode. J. Am. Chem. Soc. 2007, 129 (34), 10328–10329. doi: 10.1021/ja073643o.
(66) Bassegoda, A.; Madden, C.; Wakerley, D. W.; Reisner, E.; Hirst, J. Reversible Interconversion of CO2 and Formate by a Molybdenum-Containing Formate Dehydrogenase. J. Am. Chem. Soc. 2014, 136 (44), 15473–15476. doi: 10.1021/ja508647u.
(67) Zu, Y.; Shannon, R. J.; Hirst, J. Reversible, Electrochemical Interconversion of NADH and NAD+ by the Catalytic (Iambda) Subcomplex of Mitochondrial NADH:ubiquinone Oxidoreductase (complex I). J. Am. Chem. Soc. 2003, 125 (20), 6020–6021. doi: 10.1021/ja0343961.
(68) Kurth, J. M.; Dahl, C.; Butt, J. N. Catalytic Protein Film Electrochemistry Provides a Direct Measure of the Tetrathionate/Thiosulfate Reduction Potential. J. Am. Chem. Soc. 2015, 137 (41), 13232–13235. doi: 10.1021/jacs.5b08291.
(69) Lee, K. J.; McCarthy, B. D.; Dempsey, J. L. On Decomposition, Degradation, and Voltammetric Deviation: The Electrochemist's Field Guide to Identifying Precatalyst Transformation. Chem. Soc. Rev. 2019, 48 (11),

2927–2945. doi: 10.1039/c8cs00851e.
(70) Savéant, J.-M.; Costentin, C. Elements of Molecular and Biomolecular Electrochemistry: An Electrochemical Approach to Electron Transfer Chemistry; John Wiley & Sons, 2019.
(71) Rountree, E. S.; McCarthy, B. D.; Eisenhart, T. T.; Dempsey, J. L. Evaluation of Homogeneous Electrocatalysts by Cyclic Voltammetry. Inorg. Chem. 2014, 53 (19), 9983–10002. doi: 10.1021/ic500658x.
(72) Fourmond, V.; Léger, C. Modelling the Voltammetry of Adsorbed Enzymes and Molecular Catalysts. Current Opinion in Electrochemistry 2017, 1 (1), 110–120. doi: 10.1016/j.coelec.2016.11.002.
(73) Land, H.; Sekretareva, A.; Huang, P.; Redman, H. J.; Németh, B.; Polidori, N.; Mészáros, L. S.; Senger, M.; Stripp, S. T.; Berggren, G. Characterization of a Putative Sensory [FeFe]-Hydrogenase Provides New Insight into the Role of the Active Site Architecture. Chem. Sci. 2020, 11, 12789–12801. doi: 10.1039/D0SC03319G.
(74) Jiao, Y.; Zheng, Y.; Jaroniec, M.; Qiao, S. Z. Design of Electrocatalysts for Oxygen- and Hydrogen-Involving Energy Conversion Reactions. Chem. Soc. Rev. 2015, 44 (8), 2060–2086. doi: 10.1039/c4cs00470a.
(75) Abidi, N.; Lim, K. R. G.; Seh, Z. W.; Steinmann, S. N. Atomistic Modeling of Electrocatalysis: Are We There Yet? WIREs Comput Mol Sci 2020, 372, 145. doi: 10.1002/wcms.1499.
(76) Bard, A. J.; Faulkner, L. R. Electrochemical Methods: Fundamentals and Applications; Wiley, 2000.
(77) Appel, A. M.; Helm, M. L. Determining the Overpotential for a Molecular Electrocatalyst. ACS Catal. 2014, 4 (2), 630–633. doi: 10.1021/cs401013v.
(78) Nishiyama, M.; Higuchi, H.; Yanagida, T. Chemomechanical Coupling of the Forward and Backward Steps of Single Kinesin Molecules. Nat. Cell Biol. 2002, 4 (10), 790–797. doi: 10.1038/ncb857.
(79) Koper, M. T. M. Thermodynamic Theory of Multi-Electron Transfer Reactions: Implications for Electrocatalysis. J. Electroanal. Chem. 2011, 660 (2), 254–260. doi: 10.1016/j.jelechem.2010.10.004.
(80) Amatore, C.; Jutand, A. Mechanistic and Kinetic Studies of Palladium Catalytic Systems. J. Organomet. Chem. 1999, 576 (1-2), 254–278. doi: 10.1016/S0022-328X(98)01063-8.
(81) Kozuch, S.; Shaik, S. How to Conceptualize Catalytic Cycles? The Energetic Span Model. Acc. Chem. Res. 2011, 44 (2), 101–110. doi: 10.1021/ar1000956.
(82) Pérez-Ramírez, J.; López, N. Strategies to Break Linear Scaling Relationships. Nature Catalysis 2019, 2 (11), 971–976. doi: 10.1038/s41929-019-0376-6.
(83) Ding, Z.-B.; Maestri, M. Development and Assessment of a Criterion for the Application of Brønsted-Evans-Polanyi Relations for Dissociation Catalytic Reactions at Surfaces. Ind. Eng. Chem. Res. 2019, 58 (23), 9864–9874. doi: 10.1021/acs.iecr.9b01628.
(84) Plessow, P. N.; Abild-Pedersen, F. Examining the Linearity of Transition State Scaling Relations. J. Phys. Chem. C 2015, 119 (19), 10448–10453. doi: 10.1021/acs.jpcc.5b02055.
(85) Nørskov, J. K.; Bligaard, T.; Logadottir, A.; Bahn, S.; Hansen, L. B.; Bollinger, M.; Bengaard, H.; Hammer, B.; Sljivancanin, Z.; Mavrikakis, M.; Xu, Y.; Dahl, S.; Jacobsen, C. J. H. Universality in Heterogeneous Catalysis. J. Catal. 2002, 209 (2), 275–278. doi: 10.1006/jcat.2002.3615.
(86) Dementin, S.; Burlat, B.; Fourmond, V.; Leroux, F.; Liebgott, P.-P.; Abou Hamdan, A.; Léger, C.; Rousset, M.; Guigliarelli, B.; Bertrand, P. Rates of Intra- and Intermolecular Electron Transfers in Hydrogenase Deduced from Steady-State Activity Measurements. J. Am. Chem. Soc. 2011, 133 (26), 10211–10221. doi: 10.1021/ja202615a.
(87) Page, C. C.; Moser, C. C.; Chen, X.; Dutton, P. L. Natural Engineering Principles of Electron Tunnelling in Biological Oxidation-Reduction. Nature 1999, 402 (6757), 47–52. doi: 10.1038/46972.
(88) Ooka, H.; Nakamura, R. Shift of the Optimum Binding Energy at Higher Rates of Catalysis. J. Phys. Chem. Lett. 2019, 10 (21), 6706–6713. doi: 10.1021/acs.jpclett.9b01796.
(89) Zeradjanin, A. R.; Grote, J.-P.; Polymeros, G.; Mayrhofer, K. J. J. A Critical Review on Hydrogen Evolution Electrocatalysis: Re-Exploring the Volcano-Relationship. Electroanalysis 2016, 28 (10), 2256–2269. doi: 10.1002/elan.201600270.
(90) Rossmeisl, J.; Logadottir, A.; Nørskov, J. K. Electrolysis of Water on (oxidized) Metal Surfaces. Chem. Phys. 2005, 319 (1), 178–184. doi: 10.1016/j.chemphys.2005.05.038.
(91) Man, I. C.; Su, H.; Calle-Vallejo, F.; Hansen, H. A.; Martínez, J. I.; Inoglu, N. G.; Kitchin, J.; Jaramillo, T. F.; Nørskov, J. K.; Rossmeisl, J. Universality in Oxygen Evolution Electrocatalysis on Oxide Surfaces. ChemCatChem 2011, 3 (7), 1159–1165. doi: 10.1002/cctc.201000397.
(92) Rossmeisl, J.; Qu, Z.-W.; Zhu, H.; Kroes, G.-J.; Nørskov, J. K. Electrolysis of Water on Oxide Surfaces. J. Electroanal. Chem. 2007, 607 (1), 83–89. doi: 10.1016/j.jelechem.2006.11.008.
(93) Koper, M. T. M. Theory of Multiple Proton–electron Transfer Reactions and Its Implications for

Electrocatalysis. Chem. Sci. 2013, 4 (7), 2710–2723. doi: 10.1039/C3SC50205H.
(94) Stegelmann, C.; Andreasen, A.; Campbell, C. T. Degree of Rate Control: How Much the Energies of Intermediates and Transition States Control Rates. J. Am. Chem. Soc. 2009, 131 (23), 8077–8082. doi: 10.1021/ja9000097.
(95) Costentin, C.; Savéant, J.-M. Towards an Intelligent Design of Molecular Electrocatalysts. Nature Reviews Chemistry 2017, 1 (11), 0087. doi: 10.1038/s41570-017-0087.
(96) Sakai, K.; Hsieh, B.-C.; Maruyama, A.; Kitazumi, Y.; Shirai, O.; Kano, K. Interconversion between Formate and Hydrogen Carbonate by Tungsten-Containing Formate Dehydrogenase-Catalyzed Mediated Bioelectrocatalysis. Sensing and Bio-Sensing Research 2015, 5, 90–96. doi: 10.1016/j.sbsr.2015.07.008.
(97) Hexter, S. V.; Grey, F.; Happe, T.; Climent, V.; Armstrong, F. A. Electrocatalytic Mechanism of Reversible Hydrogen Cycling by Enzymes and Distinctions between the Major Classes of Hydrogenases. Proc. Natl. Acad. Sci. U. S. A. 2012, 109 (29), 11516–11521. doi: 10.1073/pnas.1204770109.
(98) Savéant, J.-M. Molecular Catalysis of Electrochemical Reactions. Cyclic Voltammetry of Systems Approaching Reversibility. ACS Catal. 2018, 8 (8), 7608–7611. doi: 10.1021/acscatal.8b02007.
(99) Hardt, S.; Stapf, S.; Filmon, D. T.; Birrell, J. A.; Rüdiger, O.; Fourmond, V.; Léger, C.; Plumeré, N. Reversible H2 Oxidation and Evolution by Hydrogenase Embedded in a Redox Polymer Film. Nat. Cat. 2021, 3. doi: 10.1038/s41929-021-00586-1.
(100) Fourmond, V.; Baffert, C.; Sybirna, K.; Lautier, T.; Abou Hamdan, A.; Dementin, S.; Soucaille, P.; Meynial-Salles, I.; Bottin, H.; Léger, C. Steady-State Catalytic Wave-Shapes for 2-Electron Reversible Electrocatalysts and Enzymes. J. Am. Chem. Soc. 2013, 135 (10), 3926–3938. doi: 10.1021/ja311607s.
(101) Costentin, C.; Savéant, J.-M. Multielectron, Multistep Molecular Catalysis of Electrochemical Reactions: Benchmarking of Homogeneous Catalysts. CHEMELECTROCHEM 2014, 1 (7), 1226–1236. doi: 10.1002/celc.201300263.
(102) Nicholson, R. S.; Shain, I. Theory of Stationary Electrode Polarography. Single Scan and Cyclic Methods Applied to Reversible, Irreversible, and Kinetic Systems. Anal. Chem. 1964, 36 (4), 706–723. doi: 10.1021/ac60210a007.
(103) Costentin, C.; Drouet, S.; Robert, M.; Savéant, J.-M. Turnover Numbers, Turnover Frequencies, and Overpotential in Molecular Catalysis of Electrochemical Reactions. Cyclic Voltammetry and Preparative-Scale Electrolysis. J. Am. Chem. Soc. 2012, 134 (27), 11235–11242. doi: 10.1021/ja303560c.
(104) Wang, V. C.-C.; Johnson, B. A. Interpreting the Electrocatalytic Voltammetry of Homogeneous Catalysts by the Foot of the Wave Analysis and Its Wider Implications. ACS Catal. 2019, 9 (8), 7109–7123. doi: 10.1021/acscatal.9b00850.
(105) Qian, H. A Simple Theory of Motor Protein Kinetics and Energetics. Biophys. Chem. 1997, 67 (1-3), 263–267. doi: 10.1016/S0301-4622(97)00051-3.
(106) Fisher, M. E.; Kolomeisky, A. B. Simple Mechanochemistry Describes the Dynamics of Kinesin Molecules. Proc. Natl. Acad. Sci. U. S. A. 2001, 98 (14), 7748–7753. doi: 10.1073/pnas.141080498.
(107) Brown, A. I.; Sivak, D. A. Allocating and Splitting Free Energy to Maximize Molecular Machine Flux. J. Phys. Chem. B 2018, 122 (4), 1387–1393. doi: 10.1021/acs.jpcb.7b10621.
(108) Brown, A. I.; Sivak, D. A. Allocating Dissipation across a Molecular Machine Cycle to Maximize Flux. Proc. Natl. Acad. Sci. U. S. A. 2017, 114 (42), 11057–11062. doi: 10.1073/pnas.1707534114.
(109) Fisher, M. E.; Kolomeisky, A. B. The Force Exerted by a Molecular Motor. Proc. Natl. Acad. Sci. U. S. A. 1999, 96 (12), 6597–6602. doi: 10.1073/pnas.96.12.6597.
(110) Wagoner, J. A.; Dill, K. A. Molecular Motors: Power Strokes Outperform Brownian Ratchets. J. Phys. Chem. B 2016, 120 (26), 6327–6336. doi: 10.1021/acs.jpcb.6b02776.
(111) Wilson, M. R.; Solà, J.; Carlone, A.; Goldup, S. M.; Lebrasseur, N.; Leigh, D. A. An Autonomous Chemically Fuelled Small-Molecule Motor. Nature 2016, 534 (7606), 235–240. doi: 10.1038/nature18013.
(112) Astumian, R. D. Trajectory and Cycle-Based Thermodynamics and Kinetics of Molecular Machines: The Importance of Microscopic Reversibility. Acc. Chem. Res. 2018, 51 (11), 2653–2661. doi: 10.1021/acs.accounts.8b00253.
(113) Sabatier, P. La Catalyse en chimie organique; Librairie Polytechnique, Ed.; 1913.
(114) Nørskov, J. K.; Bligaard, T.; Rossmeisl, J.; Christensen, C. H. Towards the Computational Design of Solid Catalysts. Nat. Chem. 2009, 1 (1), 37–46. doi: 10.1038/nchem.121.
(115) Quaino, P.; Juarez, F.; Santos, E.; Schmickler, W. Volcano Plots in Hydrogen Electrocatalysis - Uses and Abuses. Beilstein J. Nanotechnol. 2014, 5, 846–854. doi: 10.3762/bjnano.5.96.
(116) Costentin, C.; Savéant, J.-M. Homogeneous Molecular Catalysis of Electrochemical Reactions:

Manipulating Intrinsic and Operational Factors for Catalyst Improvement. J. Am. Chem. Soc. 2018, 140 (48), 16669–16675. doi: 10.1021/jacs.8b09154.

(117) Costentin, C.; Savéant, J.-M. Homogeneous Molecular Catalysis of Electrochemical Reactions: Catalyst Benchmarking and Optimization Strategies. J. Am. Chem. Soc. 2017, 139 (24), 8245–8250. doi: 10.1021/jacs.7b02879.

(118) Cunningham, D. W.; Barlow, J. M.; Velasquez, R. S.; Yang, J. Reversible and Selective CO2 to HCO2- Electrocatalysis near the Thermodynamic Potential. Angew. Chem. Int. Ed Engl. 2020, 59 (11), 4443–4447. doi: 10.1002/anie.201913198.

(119) Cunningham, D. W.; Yang, J. Y. Kinetic and Mechanistic Analysis of a Synthetic Reversible CO2/HCO2- Electrocatalyst. Chem. Commun. 2020, 56, 12965–12968. doi: 10.1039/d0cc05556e.

(120) Wiedner, E. S.; Chambers, M. B.; Pitman, C. L.; Bullock, R. M.; Miller, A. J. M.; Appel, A. M. Thermodynamic Hydricity of Transition Metal Hydrides. Chem. Rev. 2016, 116 (15), 8655–8692. doi: 10.1021/acs.chemrev.6b00168.

(121) Yang, J. Y.; Kerr, T. A.; Wang, X. S.; Barlow, J. M. Reducing CO2 to HCO2- at Mild Potentials: Lessons from Formate Dehydrogenase. J. Am. Chem. Soc. 2020, 142 (46), 19438–19445. doi: 10.1021/jacs.0c07965.

(122) Curtis, C. J.; Miedaner, A.; Ellis, W. W.; DuBois, D. L. Measurement of the Hydride Donor Abilities of [HM(diphosphine)2]+ Complexes (M = Ni, Pt) by Heterolytic Activation of Hydrogen. J. Am. Chem. Soc. 2002, 124 (9), 1918–1925. doi: 10.1021/ja0116829.

(123) Doherty, M. K.; Pealing, S. L.; Miles, C. S.; Moysey, R.; Taylor, P.; Walkinshaw, M. D.; Reid, G. A.; Chapman, S. K. Identification of the Active Site Acid/base Catalyst in a Bacterial Fumarate Reductase: A Kinetic and Crystallographic Study. Biochemistry 2000, 39 (35), 10695–10701. doi: 10.1021/bi000871l.

(124) Turner, K. L.; Doherty, M. K.; Heering, H. A.; Armstrong, F. A.; Reid, G. A.; Chapman, S. K. Redox Properties of Flavocytochrome c3 from Shewanella Frigidimarina NCIMB400. Biochemistry 1999, 38 (11), 3302–3309. doi: 10.1021/bi9826308.

(125) Helm, M. L.; Stewart, M. P.; Bullock, R. M.; DuBois, M. R.; DuBois, D. L. A Synthetic Nickel Electrocatalyst with a Turnover Frequency above 100,000 S^{-1} for H_2 Production. Science 2011, 333 (6044), 863–866. doi: 10.1126/science.1205864.

(126) Wilson, A. D.; Newell, R. H.; McNevin, M. J.; Muckerman, J. T.; Rakowski DuBois, M.; DuBois, D. L. Hydrogen Oxidation and Production Using Nickel-Based Molecular Catalysts with Positioned Proton Relays. J. Am. Chem. Soc. 2006, 128 (1), 358–366. doi: 10.1021/ja056442y.

(127) Le Goff, A.; Artero, V.; Jousselme, B.; Tran, P. D.; Guillet, N.; Métayé, R.; Fihri, A.; Palacin, S.; Fontecave, M. From Hydrogenases to Noble Metal-Free Catalytic Nanomaterials for H2 Production and Uptake. Science 2009, 326 (5958), 1384–1387. doi: 10.1126/science.1179773.

(128) Raugei, S.; Chen, S.; Ho, M.-H.; Ginovska-Pangovska, B.; Rousseau, R. J.; Dupuis, M.; DuBois, D. L.; Bullock, R. M. The Role of Pendant Amines in the Breaking and Forming of Molecular Hydrogen Catalyzed by Nickel Complexes. Chemistry 2012, 18 (21), 6493–6506. doi: 10.1002/chem.201103346.

(129) Rountree, E. S.; Dempsey, J. L. Potential-Dependent Electrocatalytic Pathways: Controlling Reactivity with pKa for Mechanistic Investigation of a Nickel-Based Hydrogen Evolution Catalyst. J. Am. Chem. Soc. 2015, 137 (41), 13371–13380. doi: 10.1021/jacs.5b08297.

(130) Appel, A. M.; Pool, D. H.; O'Hagan, M.; Shaw, W. J.; Yang, J. Y.; Rakowski DuBois, M.; DuBois, D. L.; Bullock, R. M. [Ni(P Ph 2 N Bn 2) 2 (CH 3 CN)] 2+ as an Electrocatalyst for H 2 Production: Dependence on Acid Strength and Isomer Distribution. ACS Catal. 2011, 1 (7), 777–785. doi: 10.1021/cs2000939.

(131) Horvath, S.; Fernandez, L. E.; Appel, A. M.; Hammes-Schiffer, S. pH-Dependent Reduction Potentials and Proton-Coupled Electron Transfer Mechanisms in Hydrogen-Producing Nickel Molecular Electrocatalysts. Inorg. Chem. 2013, 52 (7), 3643–3652. doi: 10.1021/ic302056j.

(132) Lense, S.; Dutta, A.; Roberts, J. A. S.; Shaw, W. J. A Proton Channel Allows a Hydrogen Oxidation Catalyst to Operate at a Moderate Overpotential with Water Acting as a Base. Chem. Commun. 2014, 50 (7), 792–795. doi: 10.1039/c3cc46829a.

(133) Das, P.; Ho, M.-H.; O'Hagan, M.; Shaw, W. J.; Bullock, R. M.; Raugei, S.; Helm, M. L. Controlling Proton Movement: Electrocatalytic Oxidation of Hydrogen by a nickel(II) Complex Containing Proton Relays in the Second and Outer Coordination Spheres. Dalton Trans. 2014, 43 (7), 2744–2754. doi: 10.1039/c3dt53074d.

(134) Yang, J. Y.; Smith, S. E.; Liu, T.; Dougherty, W. G.; Hoffert, W. A.; Kassel, W. S.; Rakowski DuBois, M.; DuBois, D. L.; Bullock, R. M. Two Pathways for Electrocatalytic Oxidation of Hydrogen by a Nickel

Bis(diphosphine) Complex with Pendant Amines in the Second Coordination Sphere. J. Am. Chem. Soc. 2013, 135 (26), 9700–9712. doi: 10.1021/ja400705a.

(135) Canaguier, S.; Fourmond, V.; Perotto, C. U.; Fize, J.; Pécaut, J.; Fontecave, M.; Field, M. J.; Artero, V. Catalytic Hydrogen Production by a Ni-Ru Mimic of NiFe Hydrogenases Involves a Proton-Coupled Electron Transfer Step. Chem. Commun. 2013, 49 (44), 5004–5006. doi: 10.1039/c3cc40987b.

(136) Baffert, C.; Artero, V.; Fontecave, M. Cobaloximes as Functional Models for Hydrogenases. 2. Proton Electroreduction Catalyzed by difluoroborylbis(dimethylglyoximato)cobalt(II) Complexes in Organic Media. Inorg. Chem. 2007, 46 (5), 1817–1824. doi: 10.1021/ic061625m.

(137) Frangioni, B.; Arnoux, P.; Sabaty, M.; Pignol, D.; Bertrand, P.; Guigliarelli, B.; Léger, C. In Rhodobacter Sphaeroides Respiratory Nitrate Reductase, the Kinetics of Substrate Binding Favors Intramolecular Electron Transfer. J. Am. Chem. Soc. 2004, 126 (5), 1328–1329. doi: 10.1021/ja0384072.

(138) Bertrand, P.; Frangioni, B.; Dementin, S.; Sabaty, M.; Arnoux, P.; Guigliarelli, B.; Pignol, D.; Léger, C. Effects of Slow Substrate Binding and Release in Redox Enzymes: Theory and Application to Periplasmic Nitrate Reductase. J. Phys. Chem. B 2007, 111 (34), 10300–10311. doi: 10.1021/jp074340j.

(139) Wiedner, E. S.; Brown, H. J. S.; Helm, M. L. Kinetic Analysis of Competitive Electrocatalytic Pathways: New Insights into Hydrogen Production with Nickel Electrocatalysts. J. Am. Chem. Soc. 2016, 138 (2), 604–616. doi: 10.1021/jacs.5b10853.

(140) Ho, M.-H.; Rousseau, R.; Roberts, J. A. S.; Wiedner, E. S.; Dupuis, M.; DuBois, D. L.; Bullock, R. M.; Raugei, S. Ab Initio-Based Kinetic Modeling for the Design of Molecular Catalysts: The Case of H2 Production Electrocatalysts. ACS Catal. 2015, 5 (9), 5436–5452. doi: 10.1021/acscatal.5b01152.

(141) Kitazumi, Y.; Kano, K. Bioelectrochemical and Reversible Interconversion in the Proton/Hydrogen and Carbon Dioxide/Formate Redox Systems and Its Significance in Future Energy Systems. In Electron-Based Bioscience and Biotechnology; Ishii, M., Wakai, S., Eds.; Springer Singapore: Singapore, 2020; pp 81–99. doi: 10.1007/978-981-15-4763-8_7.

(142) Chen, H.; Simoska, O.; Lim, K.; Grattieri, M.; Yuan, M.; Dong, F.; Lee, Y. S.; Beaver, K.; Weliwatte, S.; Gaffney, E. M.; Minteer, S. D. Fundamentals, Applications, and Future Directions of Bioelectrocatalysis. Chem. Rev. 2020, 120 (23), 12903–12993. doi: 10.1021/acs.chemrev.0c00472.

(143) Gallaway, J. W.; Calabrese Barton, S. A. Kinetics of Redox Polymer-Mediated Enzyme Electrodes. J. Am. Chem. Soc. 2008, 130 (26), 8527–8536. doi: 10.1021/ja0781543.

(144) Cai, R.; Minteer, S. D. Nitrogenase Bioelectrocatalysis: From Understanding Electron-Transfer Mechanisms to Energy Applications. ACS Energy Lett. 2018, 3 (11), 2736–2742. doi: 10.1021/acsenergylett.8b01637.

(145) Oughli, A. A.; Conzuelo, F.; Winkler, M.; Happe, T.; Lubitz, W.; Schuhmann, W.; Rüdiger, O.; Plumeré, N. A Redox Hydrogel Protects the O2-Sensitive [FeFe]-Hydrogenase from Chlamydomonas Reinhardtii from Oxidative Damage. Angew. Chem. Int. Ed. 2015, 54 (42), 12329–12333. doi: 10.1002/anie.201502776.

(146) Plumeré, N.; Rüdiger, O.; Oughli, A. A.; Williams, R.; Vivekananthan, J.; Pöller, S.; Schuhmann, W.; Lubitz, W. A Redox Hydrogel Protects Hydrogenase from High-Potential Deactivation and Oxygen Damage. Nat. Chem. 2014, 6 (9), 822–827. doi: 10.1038/nchem.2022.

(147) Shiraiwa, S.; So, K.; Sugimoto, Y.; Kitazumi, Y.; Shirai, O.; Nishikawa, K.; Higuchi, Y.; Kano, K. Reactivation of Standard [NiFe]-Hydrogenase and Bioelectrochemical Catalysis of Proton Reduction and Hydrogen Oxidation in a Mediated-Electron-Transfer System. Bioelectrochemistry 2018, 123, 156–161. doi: 10.1016/j.bioelechem.2018.05.003.

(148) Yuan, M.; Sahin, S.; Cai, R.; Abdellaoui, S.; Hickey, D. P.; Minteer, S. D.; Milton, R. D. Creating a Low-Potential Redox Polymer for Efficient Electroenzymatic CO2 Reduction. Angew. Chem. Int. Ed. 2018, 57 (22), 6582–6586. doi: 10.1002/anie.201803397.

(149) Szczesny, J.; Ruff, A.; Oliveira, A. R.; Pita, M.; Pereira, I. A. C.; De Lacey, A. L.; Schuhmann, W. Electroenzymatic CO2 Fixation Using Redox Polymer/Enzyme-Modified Gas Diffusion Electrodes. ACS Energy Lett. 2019, 5, 321–327. doi: 10.1021/acsenergylett.9b02436.

(150) Sakai, K.; Kitazumi, Y.; Shirai, O.; Takagi, K.; Kano, K. High-Power Formate/Dioxygen Biofuel Cell Based on Mediated Electron Transfer Type Bioelectrocatalysis. ACS Catal. 2017, 7 (9), 5668–5673. doi: 10.1021/acscatal.7b01918.

(151) Ruth, J. C.; Milton, R. D.; Gu, W.; Spormann, A. M. Enhanced Electrosynthetic Hydrogen Evolution by Hydrogenases Embedded in a Redox-Active Hydrogel. Chemistry 2020, 26 (32), 7323–7329. doi: 10.1002/chem.202000750.

(152) Tatsumi, H.; Takagi, K.; Fujita, M.; Kano, K.; Ikeda, T. Electrochemical Study of Reversible Hydrogenase

Reaction of Desulfovibrio Vulgaris Cells with Methyl Viologen as an Electron Carrier. Anal. Chem. 1999, 71 (9), 1753–1759. doi: 10.1021/ac981003l.

(153) Tsujimura, S.; Fujita, M.; Tatsumi, H.; Kano, K.; Ikeda, T. Bioelectrocatalysis-Based Dihydrogen/dioxygen Fuel Cell Operating at Physiological pH. Phys. Chem. Chem. Phys. 2001, 3 (7), 1331–1335. doi: 10.1039/B009539G.

(154) Bonitatibus, P. J., Jr; Chakraborty, S.; Doherty, M. D.; Siclovan, O.; Jones, W. D.; Soloveichik, G. L. Reversible Catalytic Dehydrogenation of Alcohols for Energy Storage. Proc. Natl. Acad. Sci. U. S. A. 2015, 112 (6), 1687–1692. doi: 10.1073/pnas.1420199112.

(155) Fujita, K.-I.; Wada, T.; Shiraishi, T. Reversible Interconversion between 2,5-Dimethylpyrazine and 2,5-Dimethylpiperazine by Iridium-Catalyzed Hydrogenation/Dehydrogenation for Efficient Hydrogen Storage. Angew. Chem. Int. Ed Engl. 2017, 56 (36), 10886–10889. doi: 10.1002/anie.201705452.

(156) Zou, Y.-Q.; von Wolff, N.; Anaby, A.; Xie, Y.; Milstein, D. Ethylene Glycol as an Efficient and Reversible Liquid Organic Hydrogen Carrier. Nat Catal 2019, 2 (5), 415–422. doi: 10.1038/s41929-019-0265-z.

(157) Xie, Y.; Hu, P.; Ben-David, Y.; Milstein, D. A Reversible Liquid Organic Hydrogen Carrier System Based on Methanol-ethylenediamine and Ethylene Urea. Angew. Chem. Weinheim Bergstr. Ger. 2019, 131 (15), 5159–5163. doi: 10.1002/ange.201901695.

(158) Shao, Z.; Li, Y.; Liu, C.; Ai, W.; Luo, S.-P.; Liu, Q. Reversible Interconversion between Methanol-Diamine and Diamide for Hydrogen Storage Based on Manganese Catalyzed (de)hydrogenation. Nat. Commun. 2020, 11 (1), 591. doi: 10.1038/s41467-020-14380-3.

(159) Boyd, R. K. Some Common Oversimplifications in Teaching Chemical Kinetics. J. Chem. Educ. 1978, 55 (2), 84. doi: 10.1021/ed055p84.

(160) Muller, P. Glossary of Terms Used in Physical Organic Chemistry (IUPAC Recommendations 1994). J. Macromol. Sci. Part A Pure Appl. Chem. 66 (5), 1077–1184. doi: 10.1351/pac199466051077.

(161) Li, H.; Buesen, D.; Dementin, S.; Léger, C.; Fourmond, V.; Plumeré, N. Complete Protection of O2-Sensitive Catalysts in Thin Films. J. Am. Chem. Soc. 2019, 141 (42), 16734–16742. doi: 10.1021/jacs.9b06790.

Acknowledgements

The authors declare no competing interests.

They acknowledge support from CNRS, Aix Marseille Université, Agence Nationale de la Recherche (ANR-15-CE05-0020), and the Excellence Initiative of Aix-Marseille University - A*MIDEX, a French “Investissements d’Avenir” programme (ANR-11-IDEX-0001-02), and the ANR-DFG project SHIELDS (PL 746/2-1). The Marseille group is part of FrenchBIC (www.frenchbic.cnrs.fr).

Display items

Box 1 **| Thousand and one meanings of the term "reversibility"**

There is no consensus about the use of the term reversibility in the context of catalysis. Our definition of "reversible catalyst", allowing the reaction to proceed quickly in response to a small departure from equilibrium[3–5] (figure 2a), is related to the meaning of "thermodynamic reversibility", which referring to near-equilibrium transformation, with no dissipation[76]. The term "efficiency" has sometimes been used with the same meaning for enzymes,[5,11] but in the context of biological motors, "efficiency" is the fraction of input free energy that is converted to output free energy (or work), irrespective of any consideration on the rate of the transformation[9].

In contrast, in homogeneous chemical kinetics and enzymology, the term "chemical reversibility" is always used to describe either what we call here a bidirectional reaction (as in the "reversible Michaelis Menten mechanism"[38])[76].

Confusion may arise between the property of a catalyst (which we describe as "(ir)reversible)") and those of the individual steps in the catalytic cycle: a step is "reversible" either if it is allowed to proceed in both directions[159], or if it fast in both directions and thus "close to equilibrium" even if the system is not. In electrochemistry for example, an electron transfer step is "electrochemically reversible" if the corresponding redox couple remains in Nernstian equilibrium with the electrode; this occurs on condition that electron transfer is very fast in both directions on the relevant time scale[76] (e.g. the voltammetric time scale, or the catalytic time scale).

The IUPAC Goldbook[160] mentions reversibility in relation to neither catalysis nor electron transfer.

Figure 1 | **Distinction between and examples of "ordered" and "branched" catalytic mechanisms.**
a | In an ordered mechanism[47], a single sequence of catalytic events occurs, clock- or counterclockwise depending on the driving force.
b | In a branched mechanism, distinct pathways can occur in the catalytic cycle (either simultaneously or in distinct ranges of driving forces).
c | The ordered mechanism of the Pt catalyst designed by J Yang, which reversibly converts CO_2 and formate. Adapted from ref [118], Wiley.
d | The generic structure of the DuBois catalyst, a mononuclear Ni complex that reversibly catalyses H_2 oxidation and evolution[4].
e | The branched mechanism proposed for H_2 oxidation and evolution by the R=Cy R'=Phe DuBois catalyst. Adapted from ref [3], American Chemical Society.
f | The multiple pathways in the five-states branched mechanism of the motor kinesin[28]. The triangles are the two microtubule binding domains. The green arrows show the catalytic cycle that leads to forward movement (to the right). The black arrows show a futile cycle that produces no work. The red arrows show the backward step, which prevails when an external backward force is applied. In this model all four cycles hydrolyse ATP.

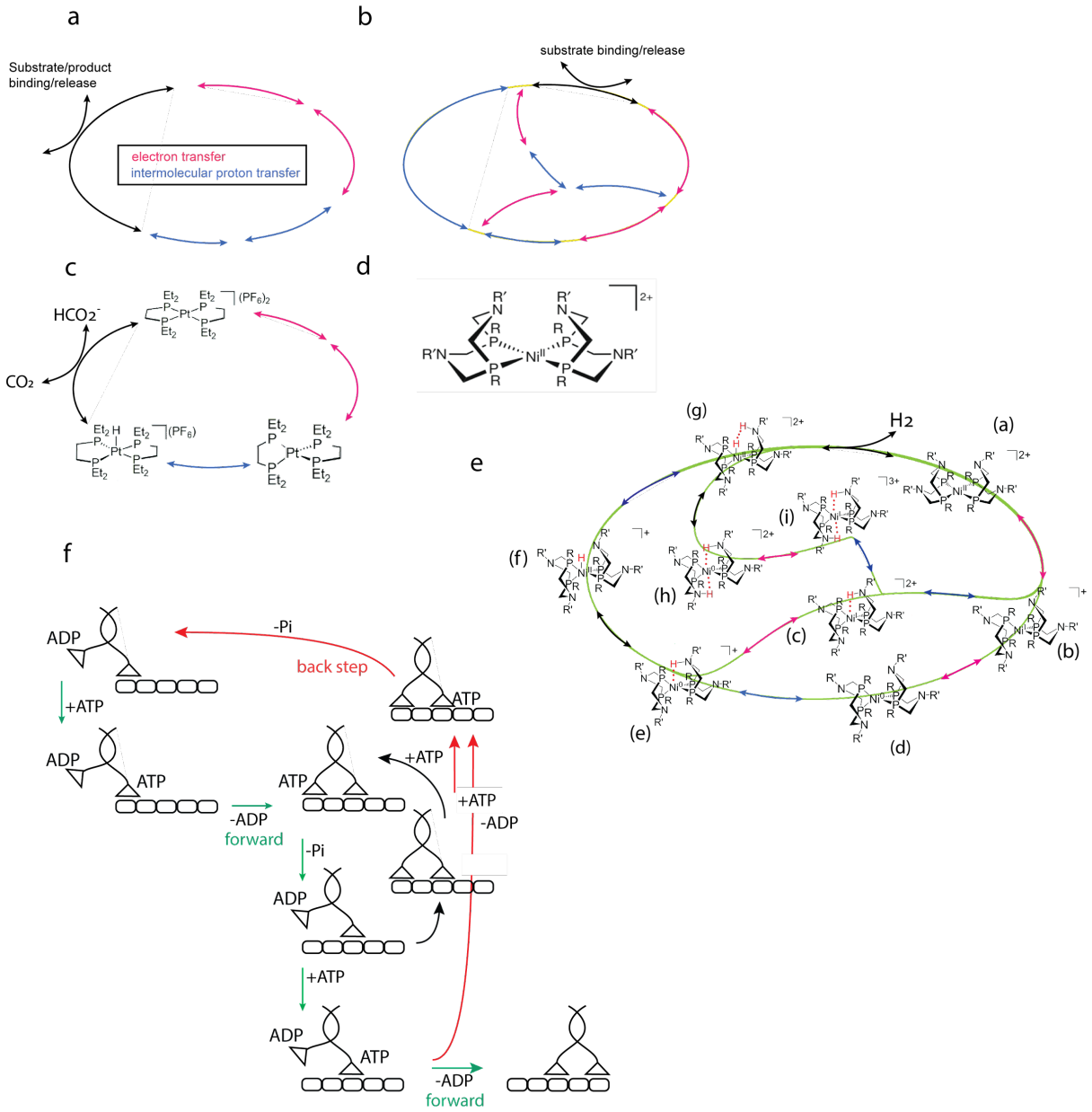
a
Substrate/product binding/release
electron transfer
intermolecular proton transfer
b
substrate binding/release
c
HCO2-
CO2
d
e
H2
(a)
(b)
(c)
(d)
(e)
(f)
(g)
(h)
(i)
f
ADP
ATP
-Pi
back step
+ATP
-ADP
forward

Figure 2 | **Reversibility in catalysis.**

a | Illustration that the free energy of a reaction sets the direction of the reaction, not its rate. ξ is the extent of reaction.

b | A rare example of control of the driving force in homogeneous kinetics: the rate of H_2 evolution by hydrogenase as a function of the Nernst potential of the MVox/red couple used as its redox partner (replotted from ref [57], Wiley).

c | The velocity of kinesin at constant ATP concentration, as a function of the backward force (replotted from ref [28], Springer Nature Limited).

d-h | Various electrochemical configurations (d: catalyst diffusing in solution[3,98], e: catalyst grafted onto a surface[3,127], f: enzyme adsorbed onto a surface[13,72], g: enzyme entrapped into a redox polymer film[99,161], h: electrocatalyst or "surface catalyst").

i | Typical current potential response of an irreversible molecular catalyst.

j | Typical current/potential response of a reversible molecular catalyst.

k | Typical reversible current/potential response of a surface catalyst.

l | Bidirectional irreversible H^+/H_2 transformation by the R=cyclohexyl, R'=pyridizine DuBois catalyst in wet acetonitrile (replotted from the data in ref [41], Wiley). The reductive peak at low potential reveals a deviation from steady-state which we do not discuss.

m | Reversible H^+/H_2 transformation by the R=cyclohexyl, R'=phenyl DuBois catalyst in acidic methanol in the presence of water, 0.25 atm. of H_2, 25°C. Replotted from ref [42], American Chemical Society.

n | Reversible H^+/H_2 transformation by FeFe hydrogenase entrapped into a redox polymer film, under conditions of mediated electron transfer (MET), pH 7.6, 1 atm. of H_2 (replotted from the data in ref [99], Springer Nature Limited).

o | Speed-efficiency trade-offs of various biological motors, Na-K ATPase (square), F_1 ATP-synthase (triangles), kinesin (circles)[58]. The thermodynamic driving force is $\Delta\mu(1-\eta)$ (where $\Delta\mu$ is the input free energy and η is the efficiency). In panels o to u, the colors violet and orange indicate irreversible and reversible responses, respectively. (Replotted from the data in ref [58], National Academy of Sciences.)

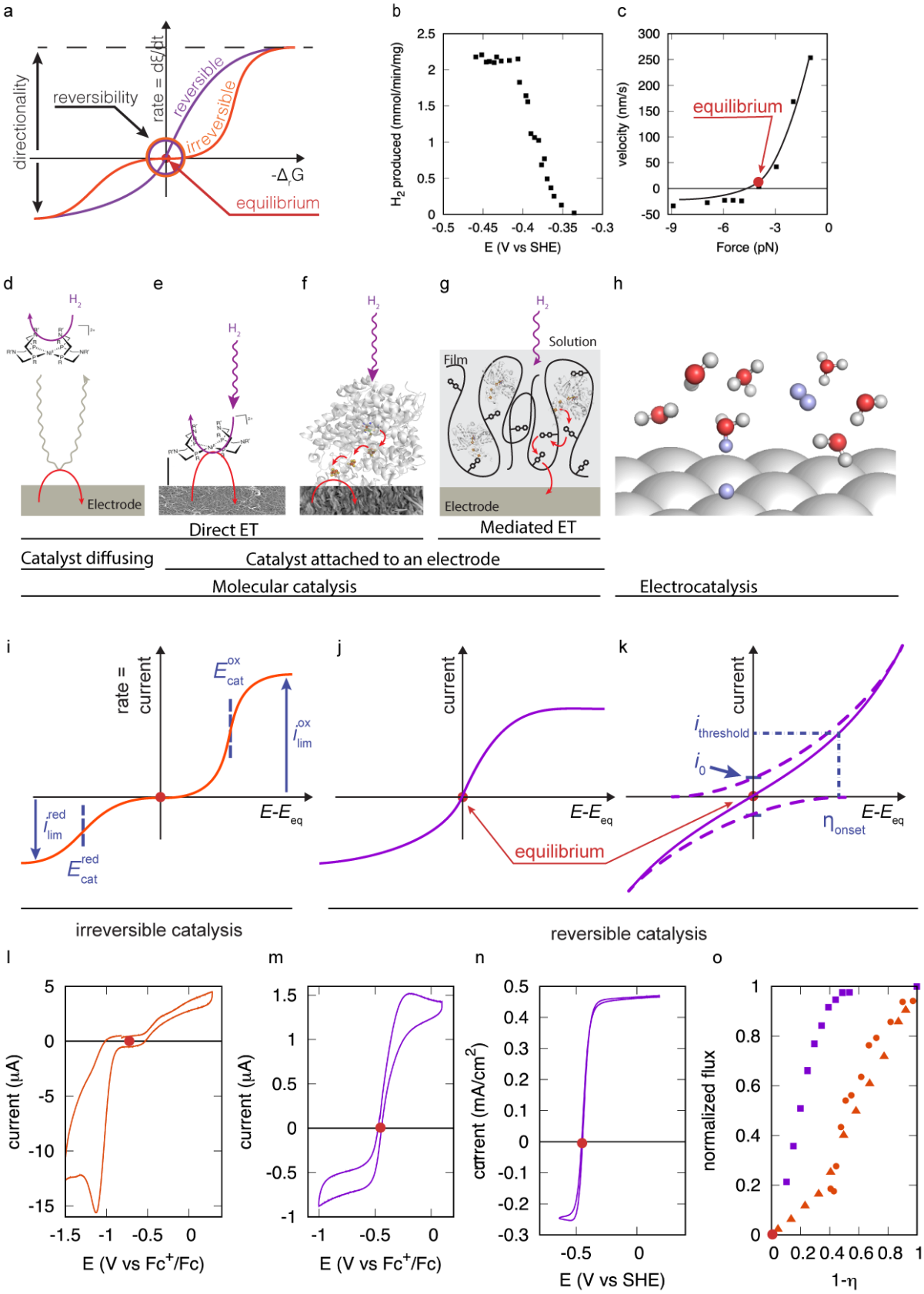
a
directionality
reversibility
rate = dξ/dt
reversible
irreversible
equilibrium
-ΔrG
b
H2 produced (mmol/min/mg)
E (V vs SHE)
c
velocity (nm/s)
equilibrium
Force (pN)
d
e
f
g
h
Electrode
Direct ET
Film
Solution
Mediated ET
Catalyst diffusing
Catalyst attached to an electrode
Molecular catalysis
Electrocatalysis
i
rate = current
E-Eeq
irreversible catalysis
j
current
equilibrium
reversible catalysis
k
current
ithreshold
i0
ηonset
l
current (µA)
E (V vs Fc+/Fc)
m
n
current (mA/cm2)
E (V vs SHE)
o
normalized flux
1-η

This is a post-peer-review, pre-copyedit version of an article in press. Please cite: Fourmond, V., Plumeré, N & Léger, C. Reversible catalysis. Nat. Rev. Chem. doi: 10.1038/s41570-021-00268-3 (2021)

Figure 3 **| The power output of motors and fuel cells**

a | The structure of the kinesin dimer, indicating the direction of forward motion and of the backward force that can be applied to slow the motion. Kinesin moves toward the "plus end" of the microtubule, making steps of length *L* (8nm) every τ seconds (figure adapted from https://pdb101.rcsb.org/motm/64).

b | The power ($P=FL/\tau$) that is produced as a function of the magnitude of this force (replotted from the data in ref [78]).

c | A schematic representation of a fuel cell.

d | Typical evaluation of the performance of a fuel cell (replotted from the data in ref [99]): increasing the load of the fuel cell (the resistance of the outer circuit), increases the voltage *U* and decreases the current *i*. The power is the product of the two. Note the sharp increase in current as the resistance is decreased to allow electron flow. Here the residual free energy that is dissipated even at low current results for an overpotential at the cathode. These data were acquired with a two-compartment fuel cell: the H_2-oxidizing anode was made of a flat glassy carbon electrode supporting a redox film of polymer embedding a FeFe hydrogenase (larger *j* and *P* are obtained with this kind of film supported on a high surface area gas breathing electrode); the O_2 reducing cathode consisted of bilirubin oxidase immobilized on a high surface Toray paper electrode. The observed open circuit voltage value (1.16 V) is close to the thermodynamic limit (1.23 V), with the residual overpotential resulting from the ORR[99].